

Supplementary Information for

**Relatively stable pressure effects and time-increasing thermal contraction  
control Heber geothermal field displacement**

Guoyan Jiang<sup>1\*</sup>, Andrew J. Barbour<sup>2\*</sup>, Robert J. Skoumal<sup>3</sup>, Kathryn Materna<sup>3</sup>, Joshua Taron<sup>3</sup> & Aren  
Crandall-Bear<sup>4</sup>

<sup>1</sup>School of Geodesy and Geomatics, Hubei LuoJia Laboratory, Wuhan University, Wuhan, China <sup>2</sup>US  
Geological Survey, Vancouver, WA, USA. <sup>3</sup>US Geological Survey, Moffett Field, CA, USA. <sup>4</sup>University  
of Nevada, Reno, NV, USA.

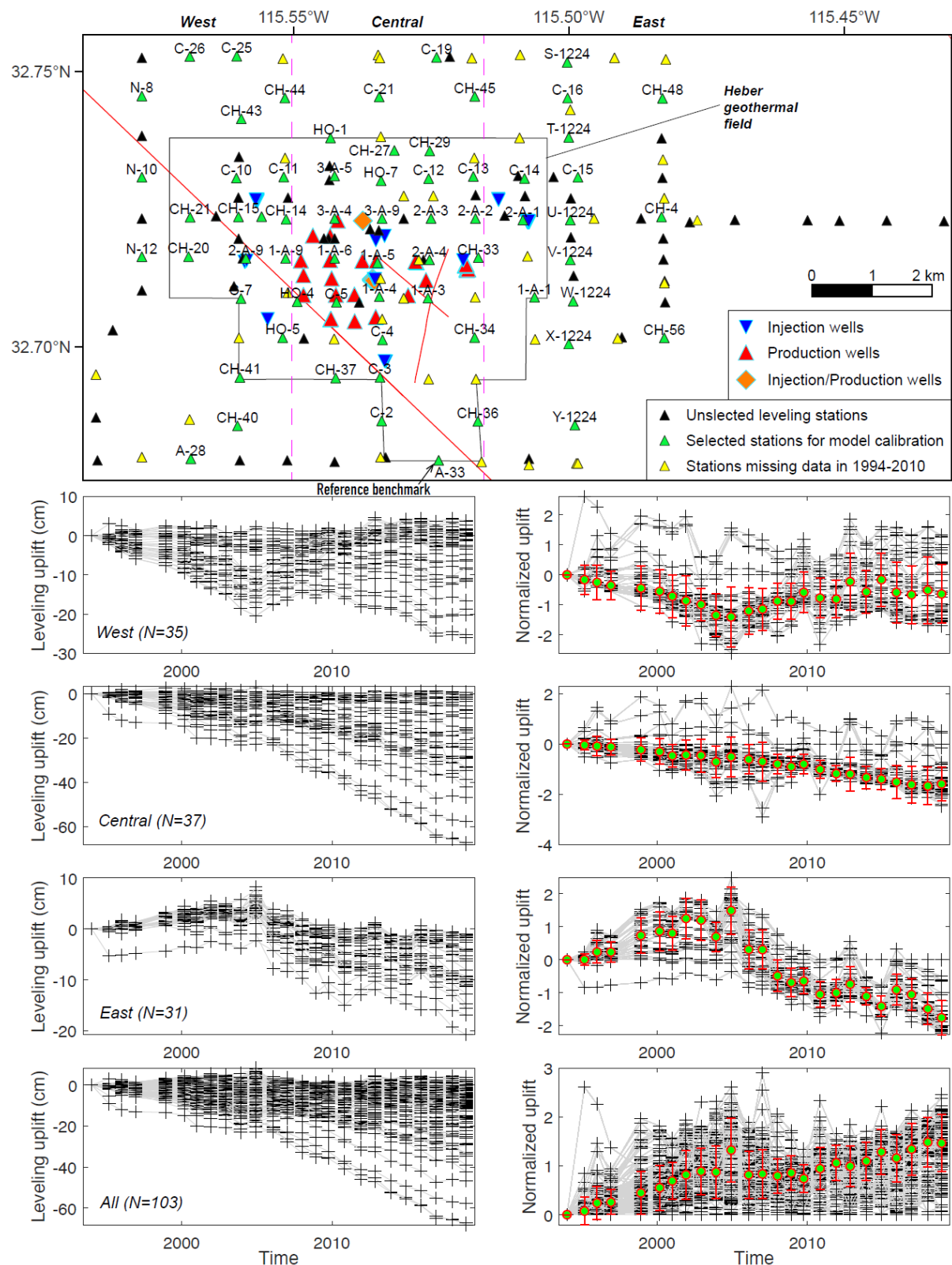
\*Corresponding author. E-mail: [gyjiang@whu.edu.cn](mailto:gyjiang@whu.edu.cn)(G.J.); [abarbour@usgs.gov](mailto:abarbour@usgs.gov)(A.J.B.)

**This PDF file includes:**

Supplementary Figs. 1 to 24

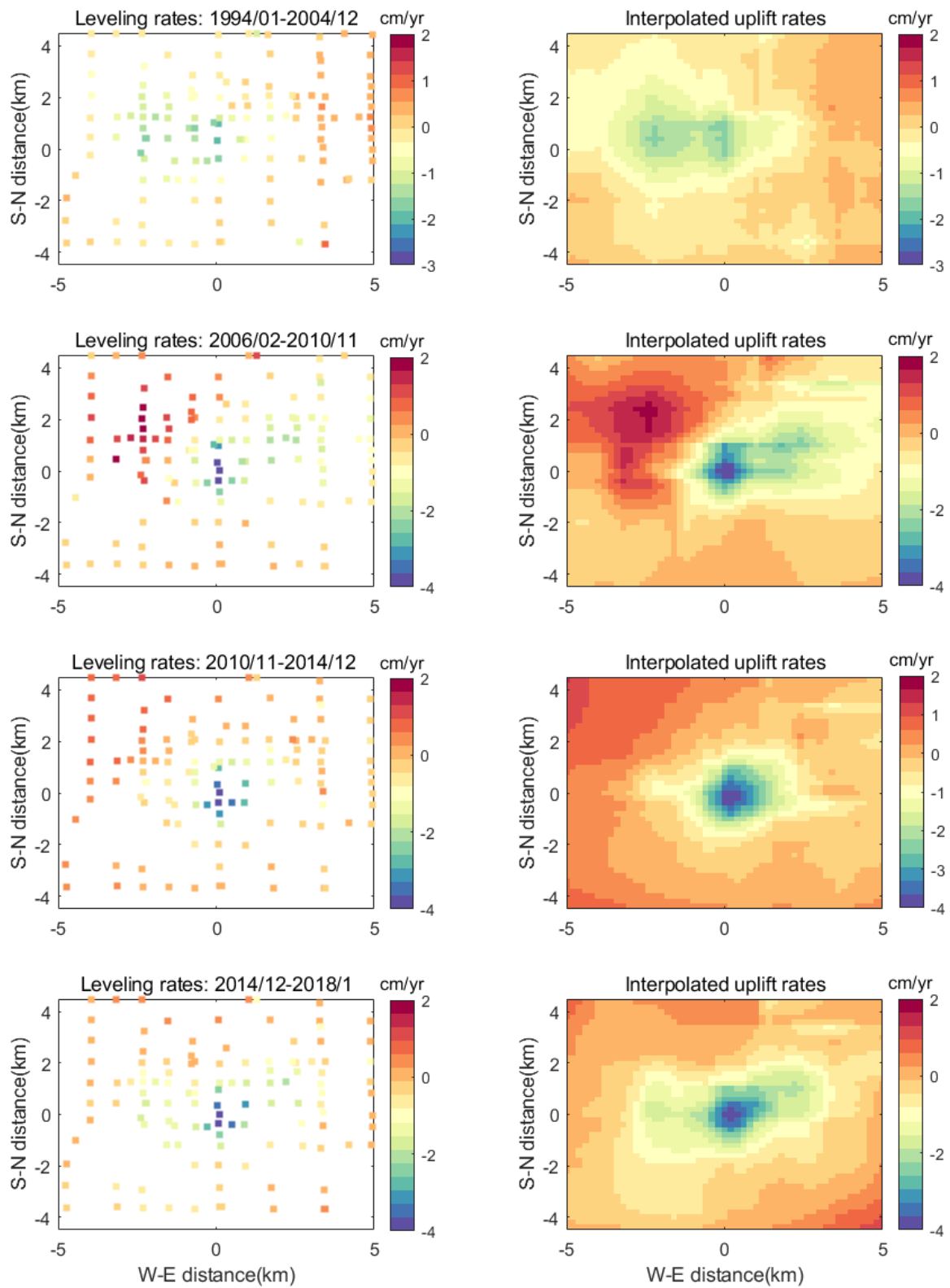
Supplementary Tables 1 to 17

## Supplementary figures

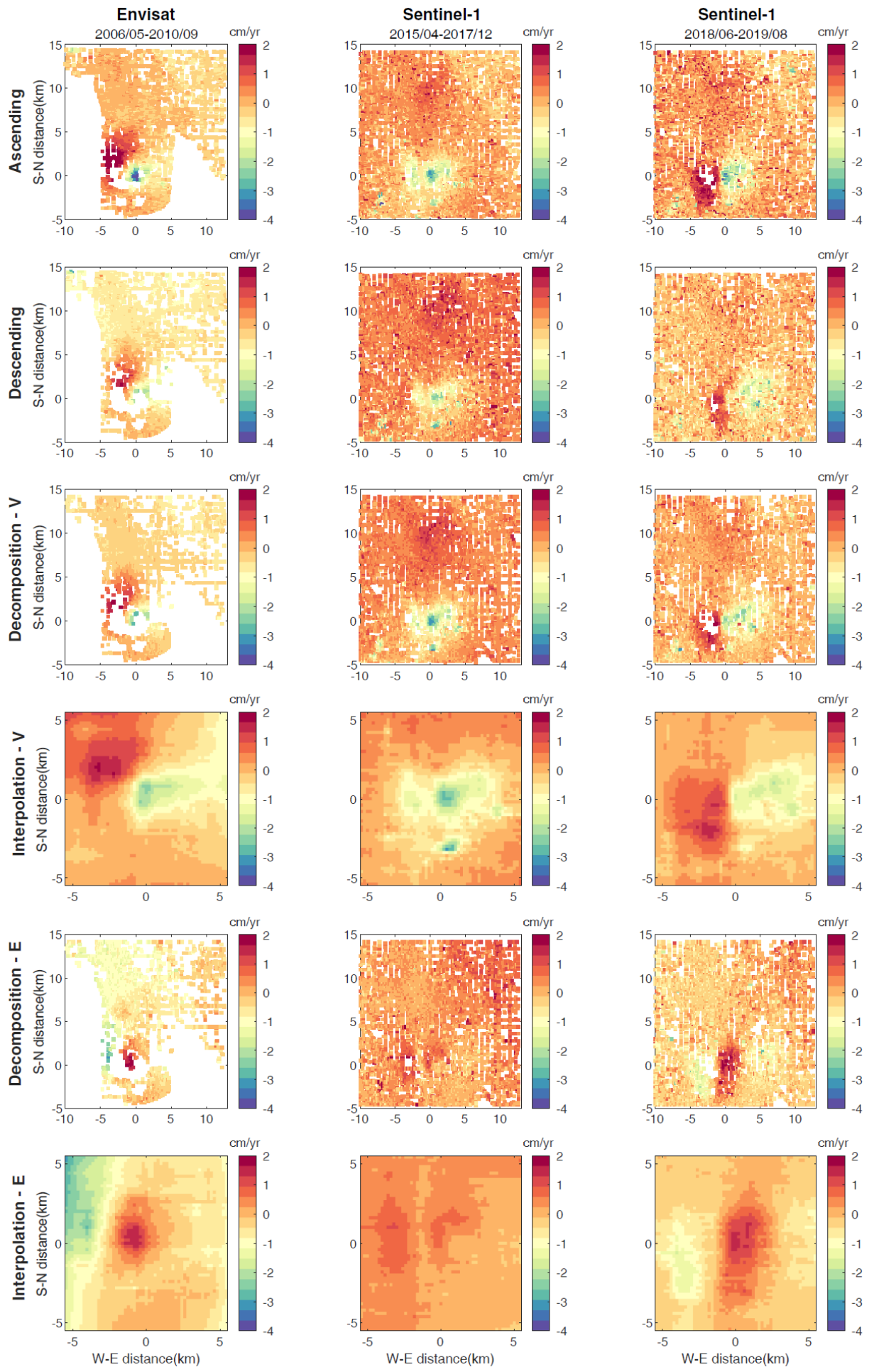


**Supplementary Fig. 1. Spatial distribution of leveling stations and time series of observed vertical displacement.** The study area is divided into three zones: west, central and east. There are only injection wells in the west and east zones. Two panels of the 2<sup>nd</sup> row show the observed and normalized displacement time series of 35 leveling benchmarks without missing data in the west zone, respectively. The red bars reflect the variability in the normalized leveling time series rather than observation errors. The 3<sup>rd</sup>

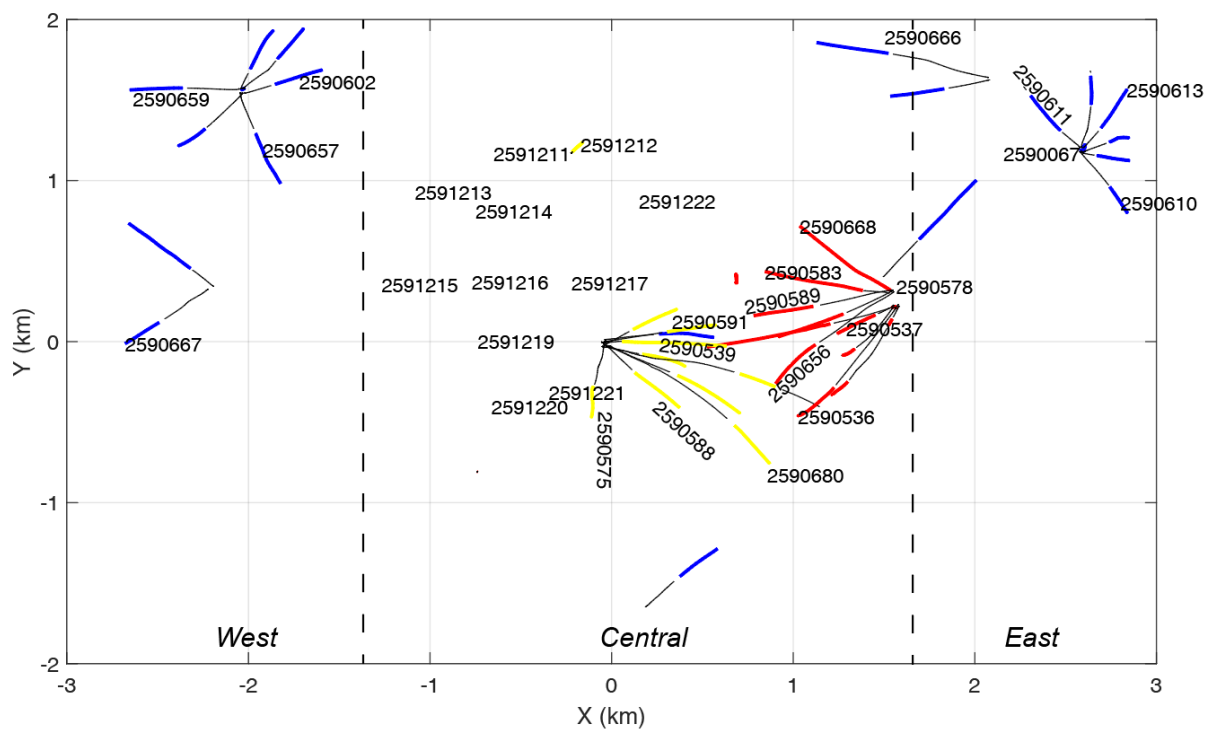
row presents the displacement time series of 37 benchmarks without missing data in the central zone. The 4<sup>th</sup> row shows the displacement time series of 31 benchmarks without missing data in the east zone. The bottom row shows the time series of 103 benchmarks without missing data in the study area.



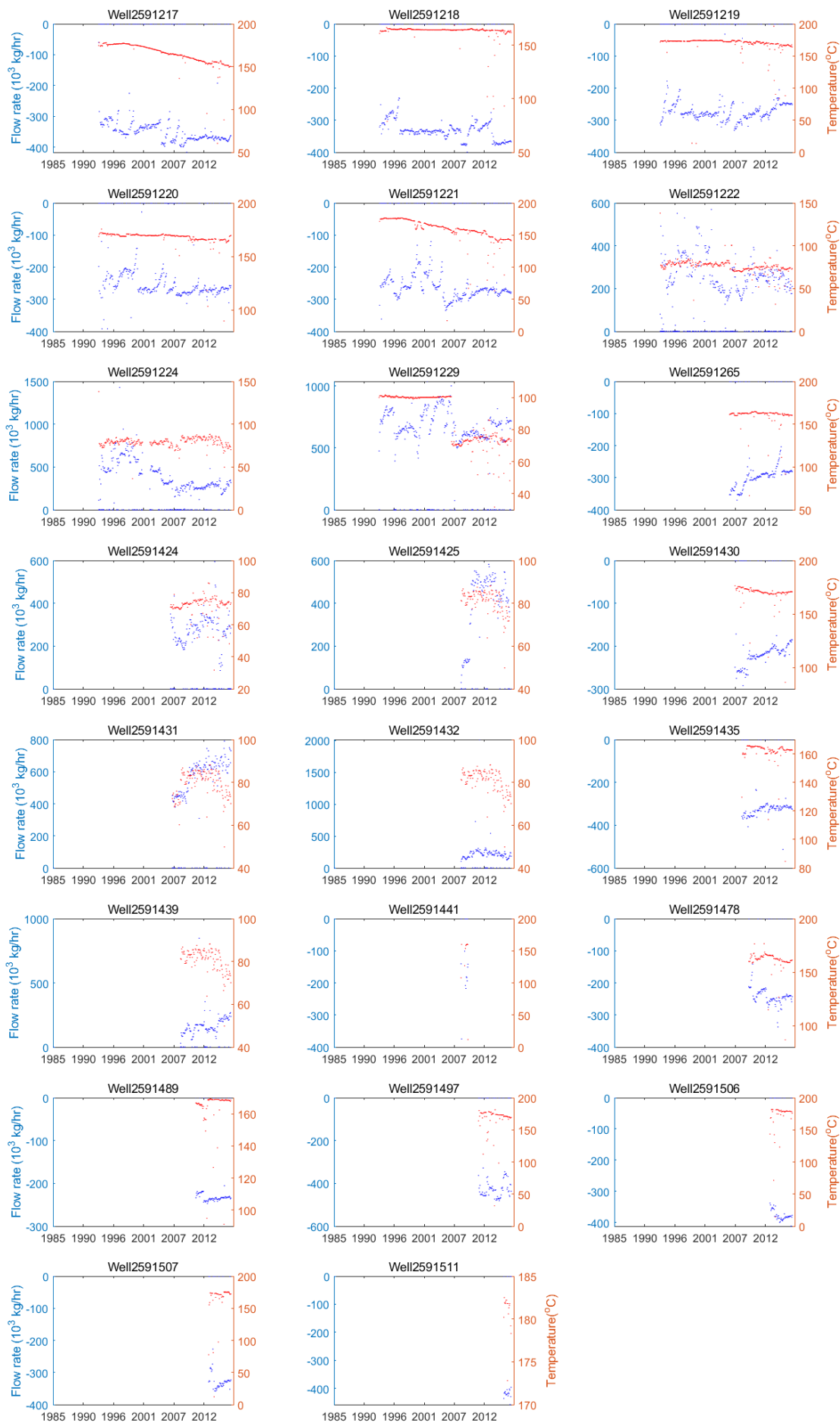
**Supplementary Fig. 2. Vertical displacement rates of four time periods observed by leveling benchmarks.** Four panels of the left column show the displacement rate at each benchmark. The right column shows the corresponding displacement rate maps derived from interpolation with the Kriging method (*Lophaven et al., 2002*).



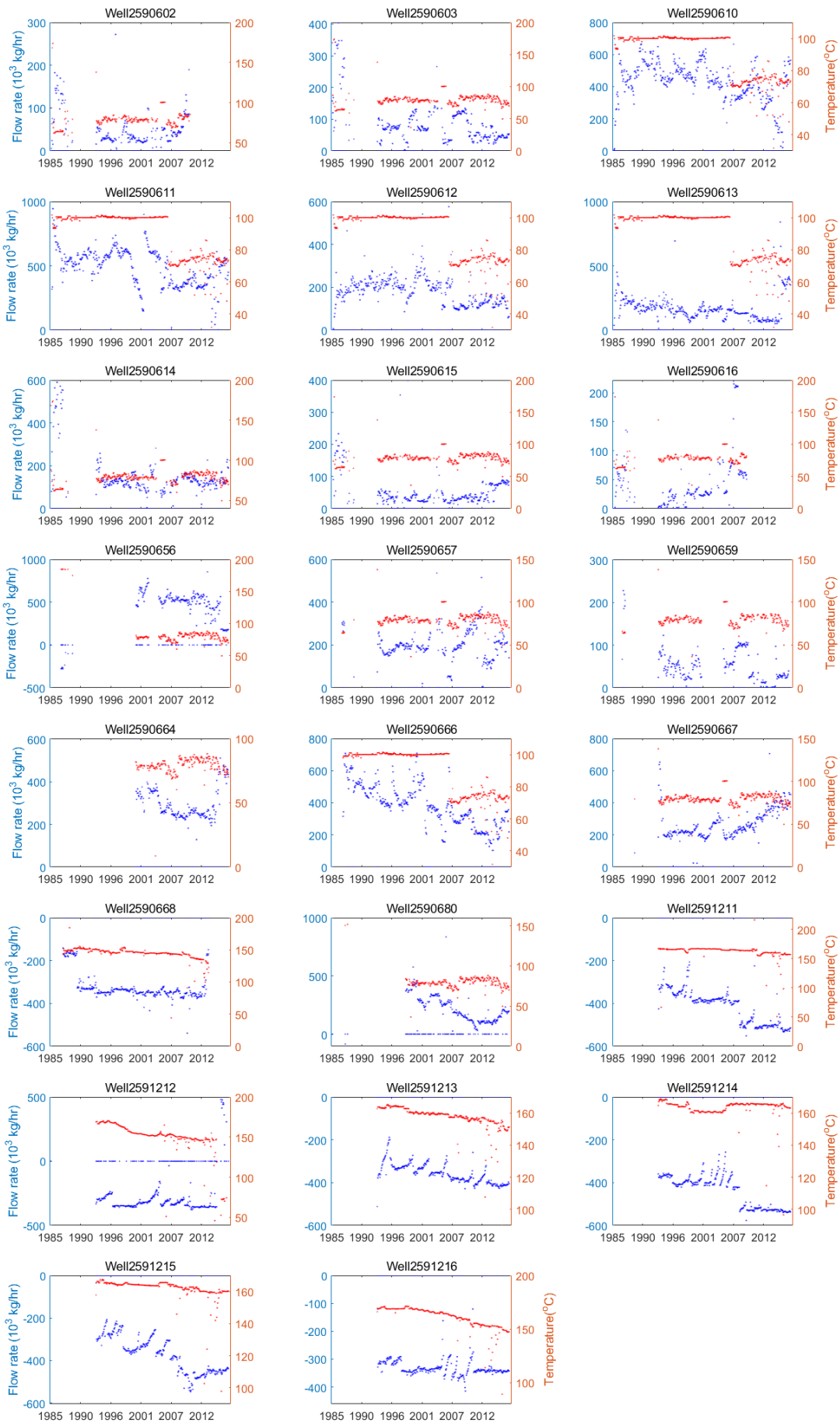
**Supplementary Fig. 3. InSAR measured surface displacement rates.** The displacement within three time periods is first measured with the ascending and descending track SAR images of the Envisat and Sentinel-1 satellites in the line-of-sight (LOS) direction and then decomposed into the vertical and eastern components. Note the change in spatial scales between the observed and interpolated results.



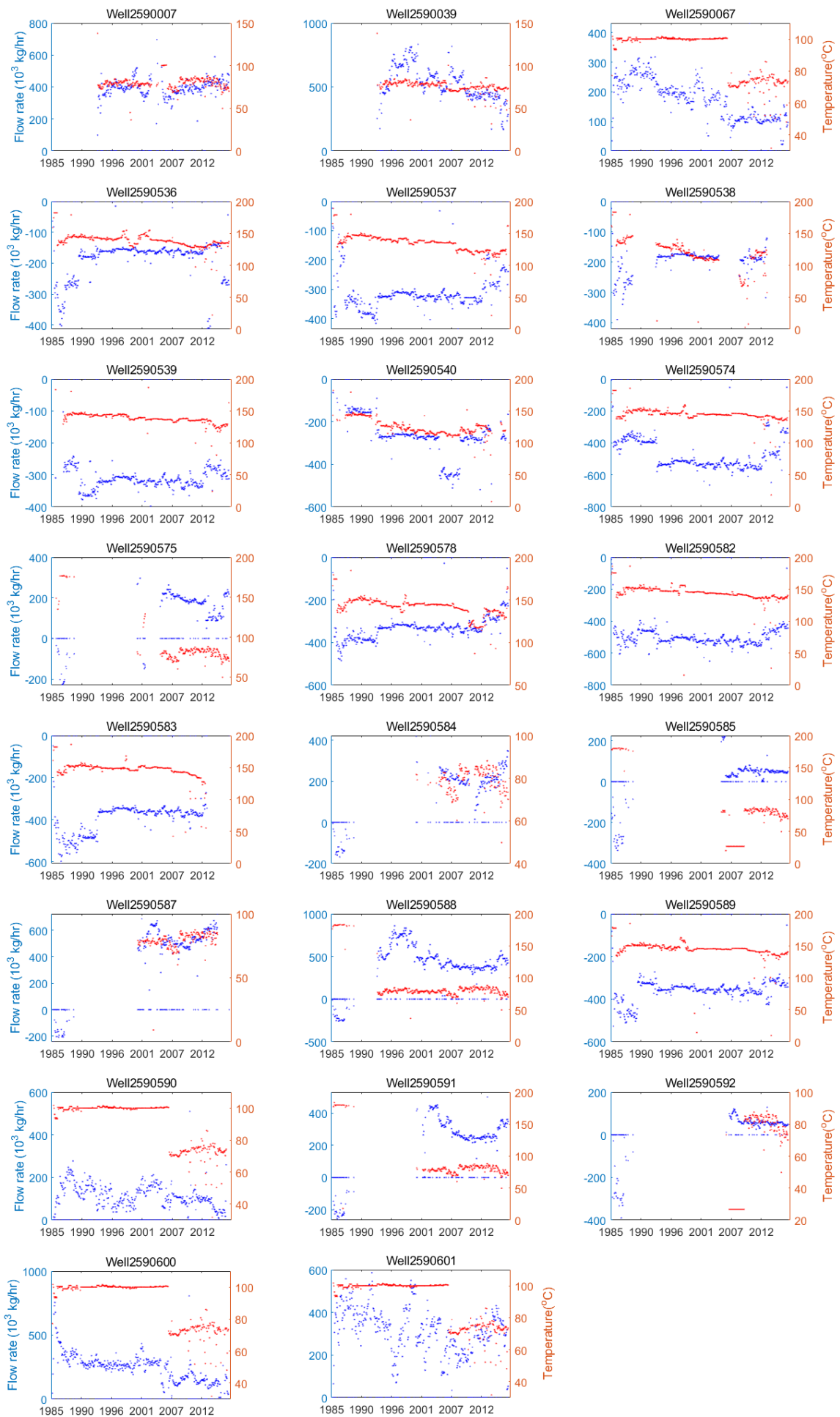
**Supplementary Fig. 4. Top view of the trajectories of operation wells within the HGF.** Blue color marks the open-hole sections of injection wells. Red color labels the open-hole sections of extraction wells. Yellow color shows the open-hole sections of 10 wells that were first completed for extraction and later converted to injection. The wells selected for model calibration are labeled with their California API IDs.



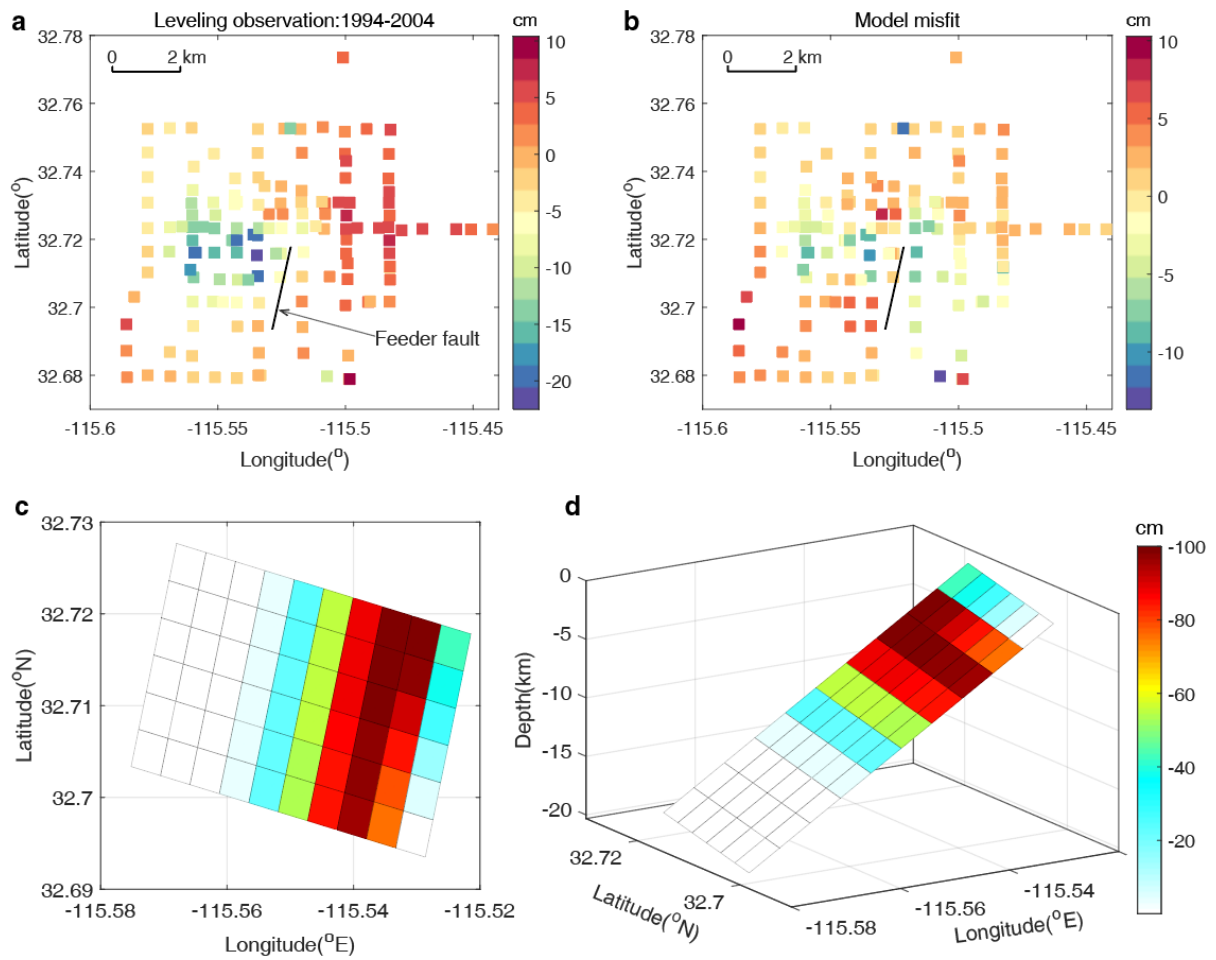
**Supplementary Fig. 5. Production rates (blue) and temperature records (red) of 69 wells.**



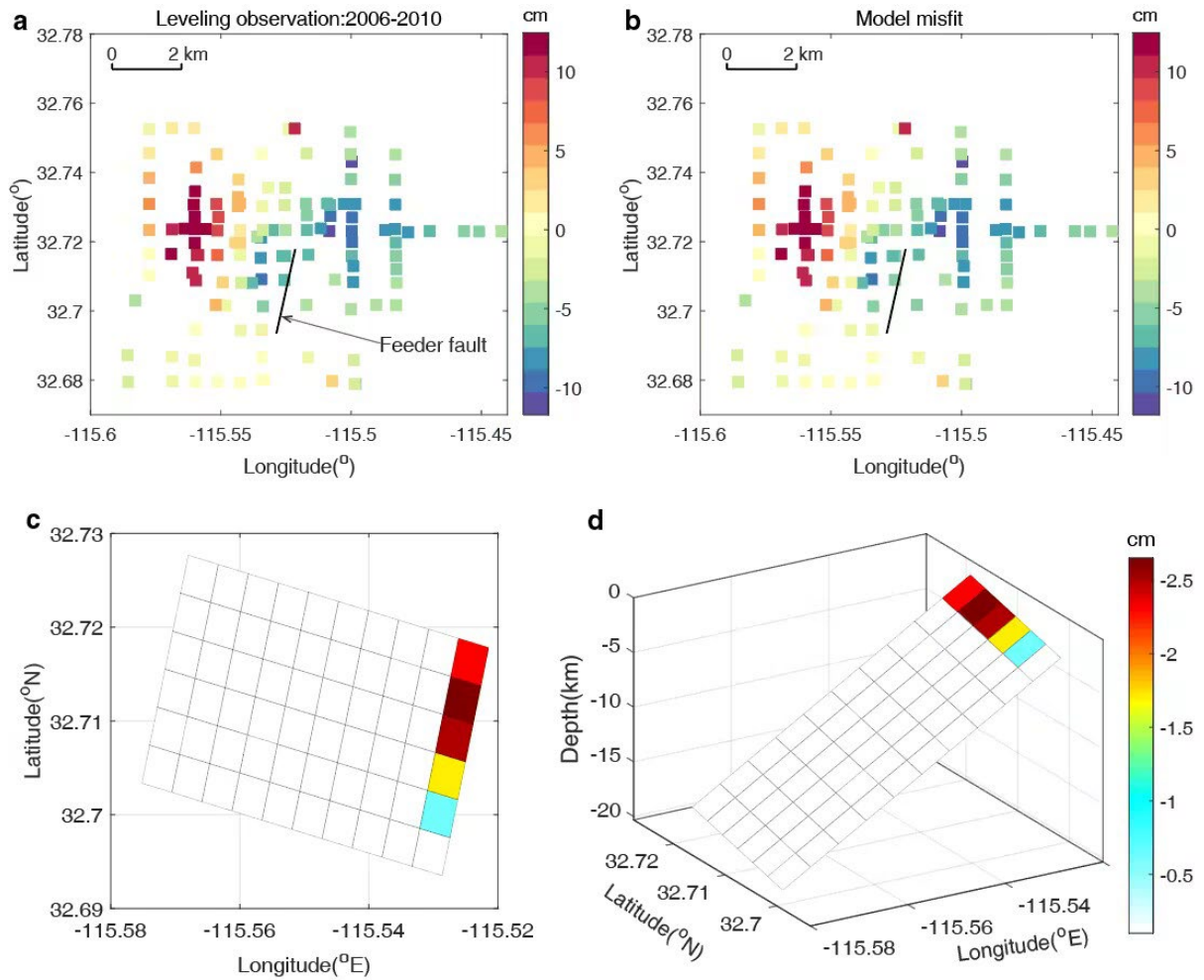
Supplementary Fig. 5. Continued.



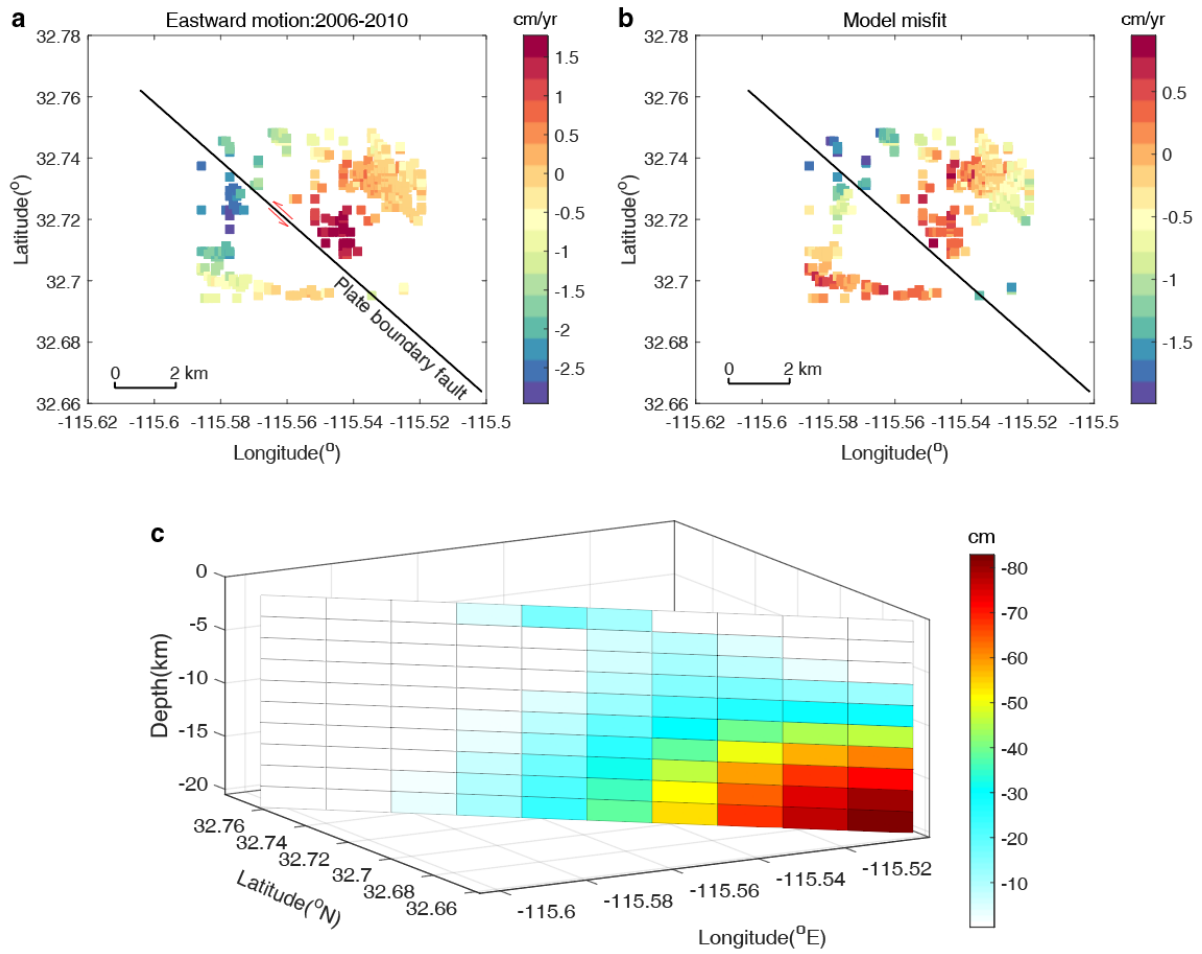
Supplementary Fig. 5. Continued.



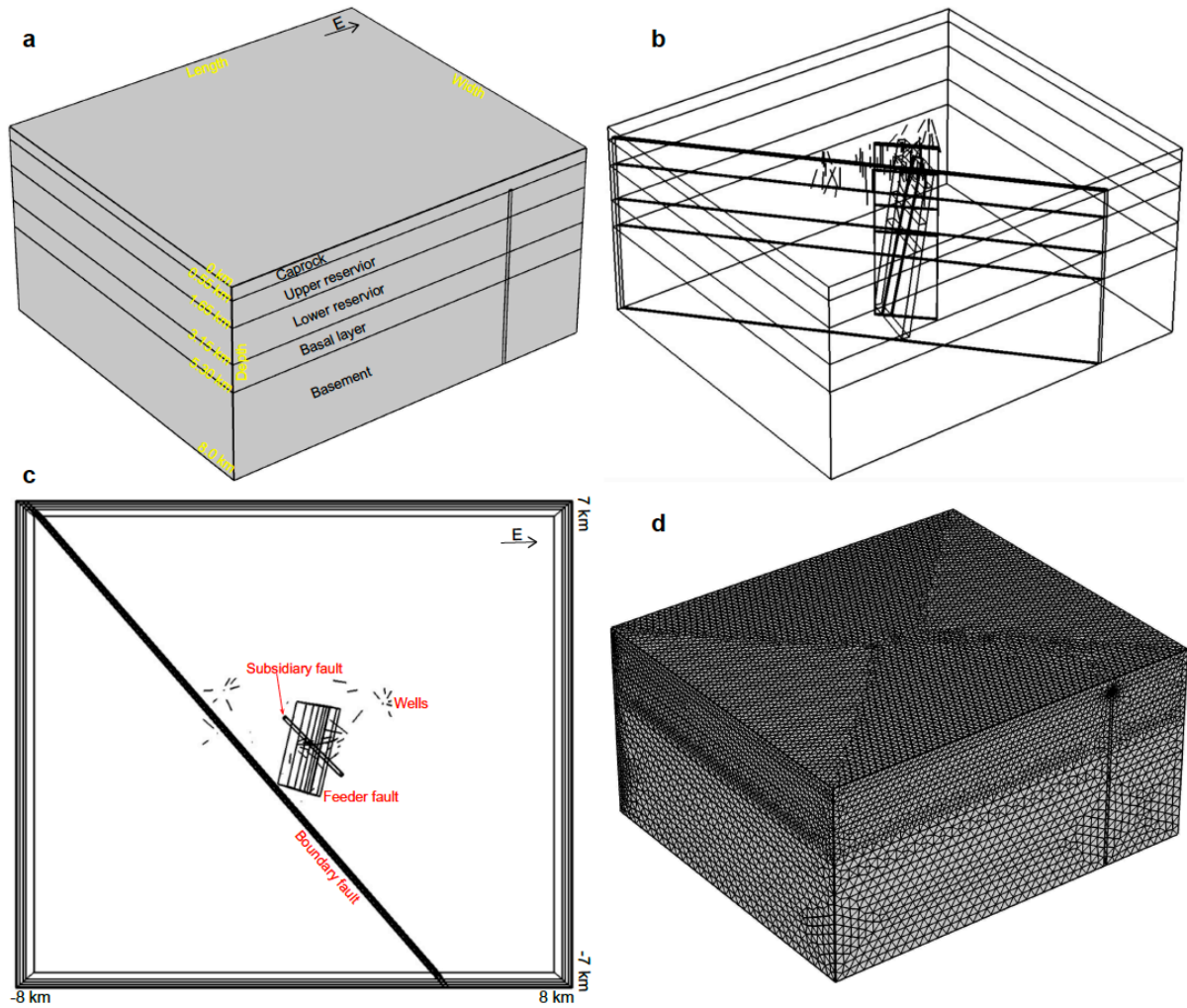
**Supplementary Fig. 6. Fault modeling of long-term vertical surface displacement from 1994 to 2004.** **a** Leveling observed surface displacement from January 1994 to December 2004. **b** Misfit between leveling observations and predictions with the inverted slip distribution on the normal-slip feeder fault shown in **c** (2D view) and **d** (3D view). Negative values represent normal slip.



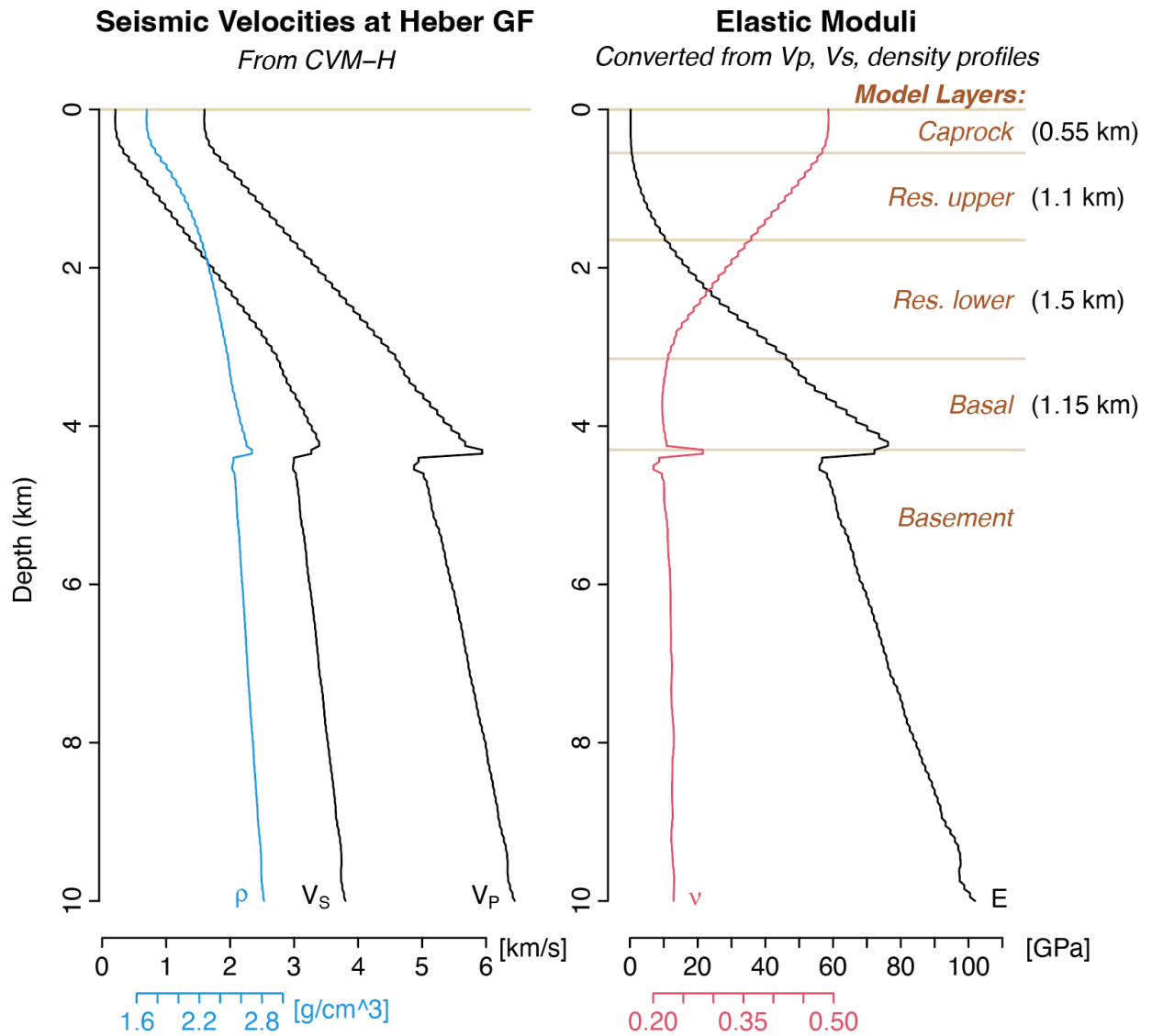
**Supplementary Fig. 7. Fault modeling of vertical transient displacement from 2006 to 2010. a** Corrected leveling displacement with removing the long-term displacement trends observed before 2005. **b** Misfit between leveling observations and predictions with the inverted slip distribution on the normal-slip feeder fault shown in **c** (2D view) and **d** (3D view). Negative values represent normal slip.



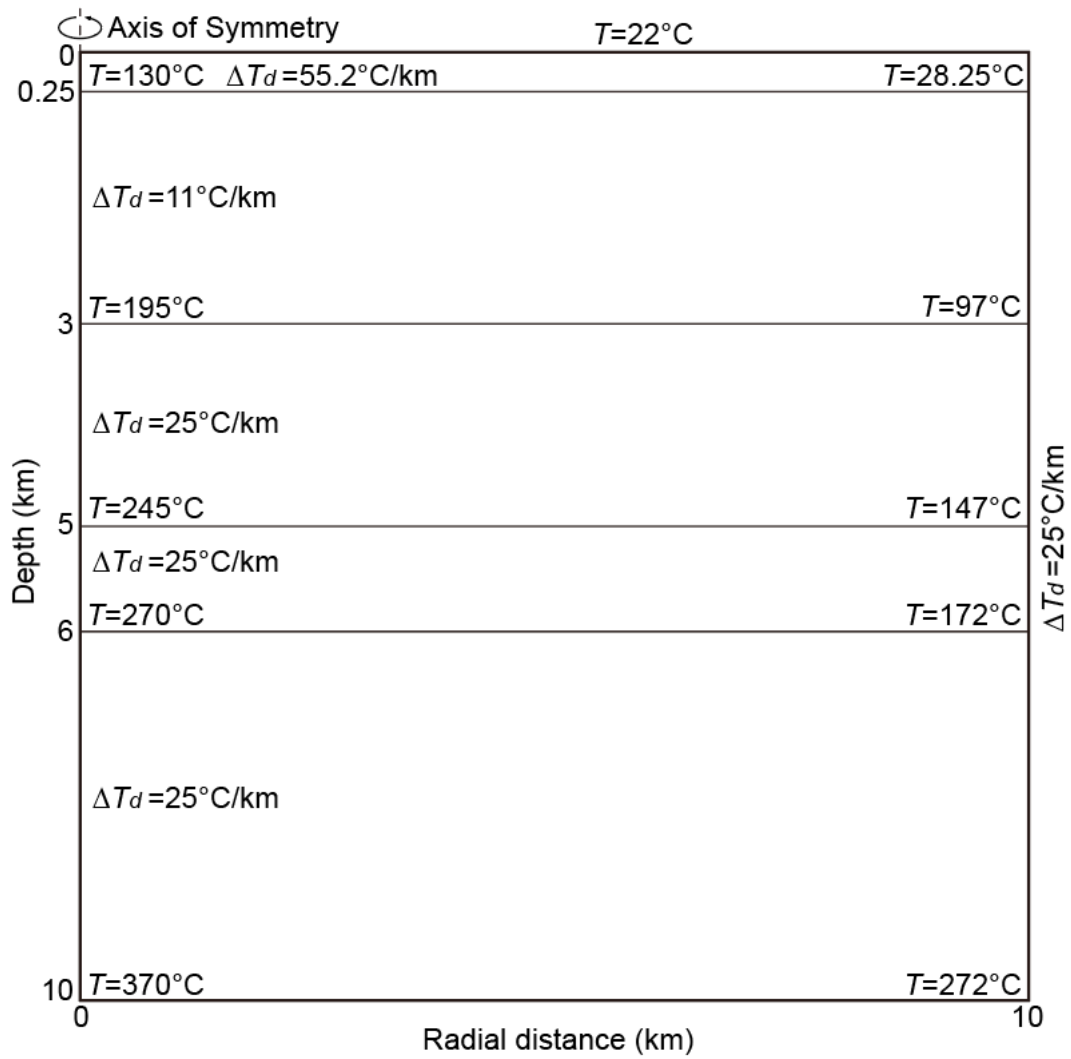
**Supplementary Fig. 8. Fault modeling of the eastward surface displacement from 2006 to 2010 derived from InSAR observations. a** Observed surface displacement in the east direction. **b** Misfit between leveling observations and predictions with the inverted slip distribution on the strike-slip plate boundary fault shown in **c**. Negative values represent right-lateral slip.



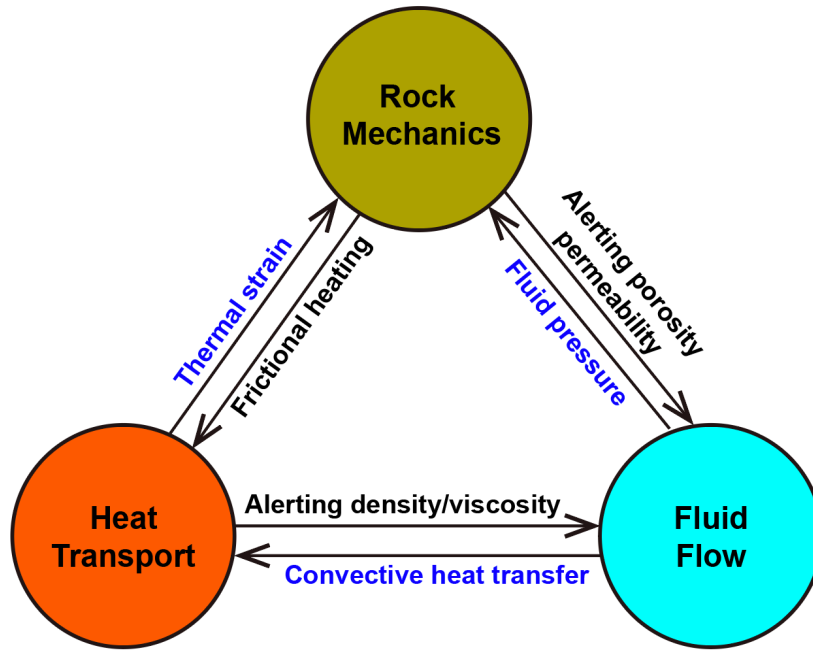
**Supplementary Fig. 9. 3D geometrical model of the HGF. a** Stratigraphic division; **b** Perspective view; **c** Top view with faults and wells labeled; **d** Tetrahedral model mesh.



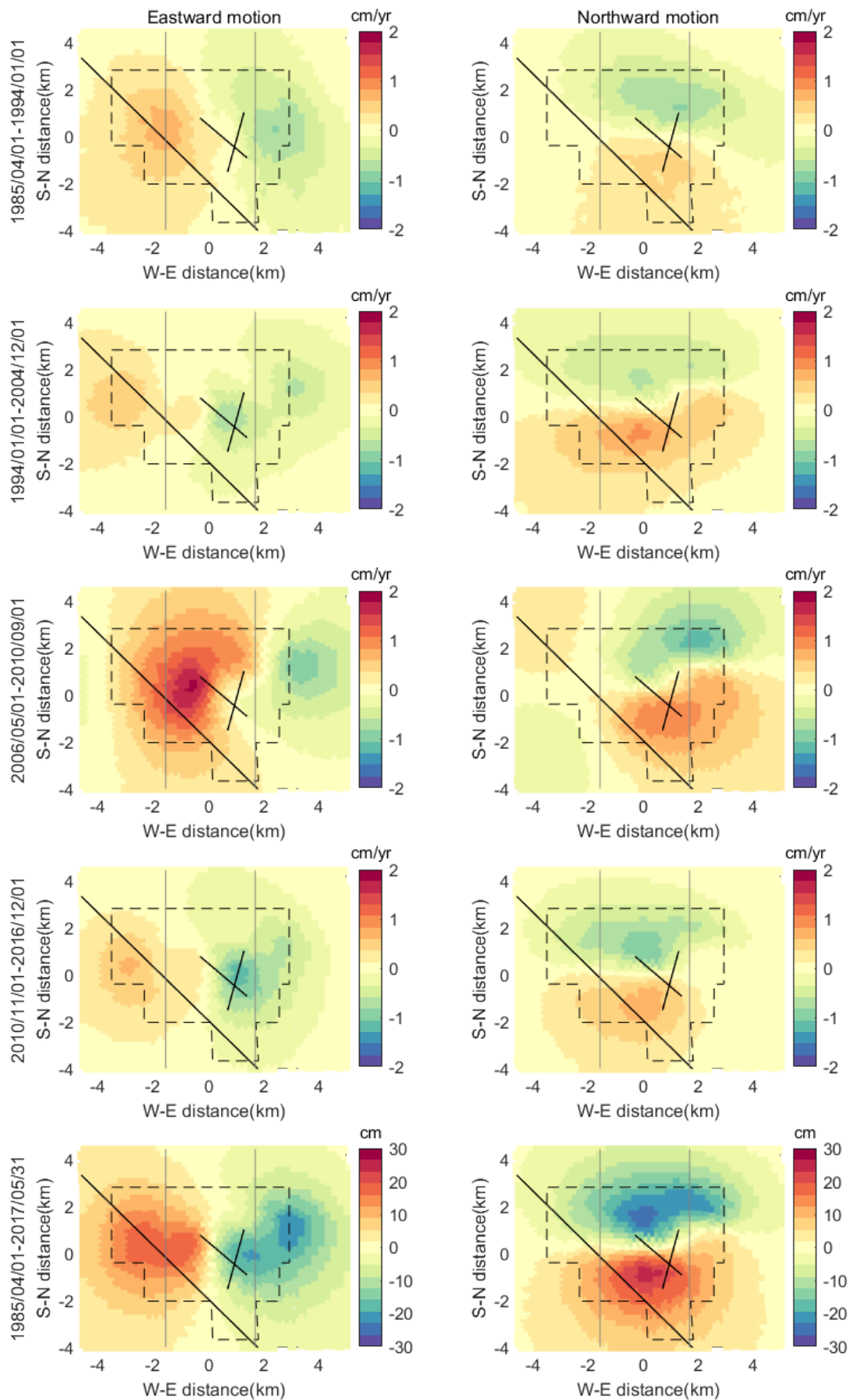
**Supplementary Fig. 10.** Profiles of seismic velocities ( $V_p$  and  $V_s$ ) and density ( $\rho$ ) at the HGF (left) converted to Poisson ratio ( $\nu$ ) and Young's modulus ( $E$ ) (right). The velocities are from the SCEC Community Velocity Model-Harvard (CVM-H) (*Shaw et al., 2015*). The depths of the five model layer interfaces are shown as horizontal lines.



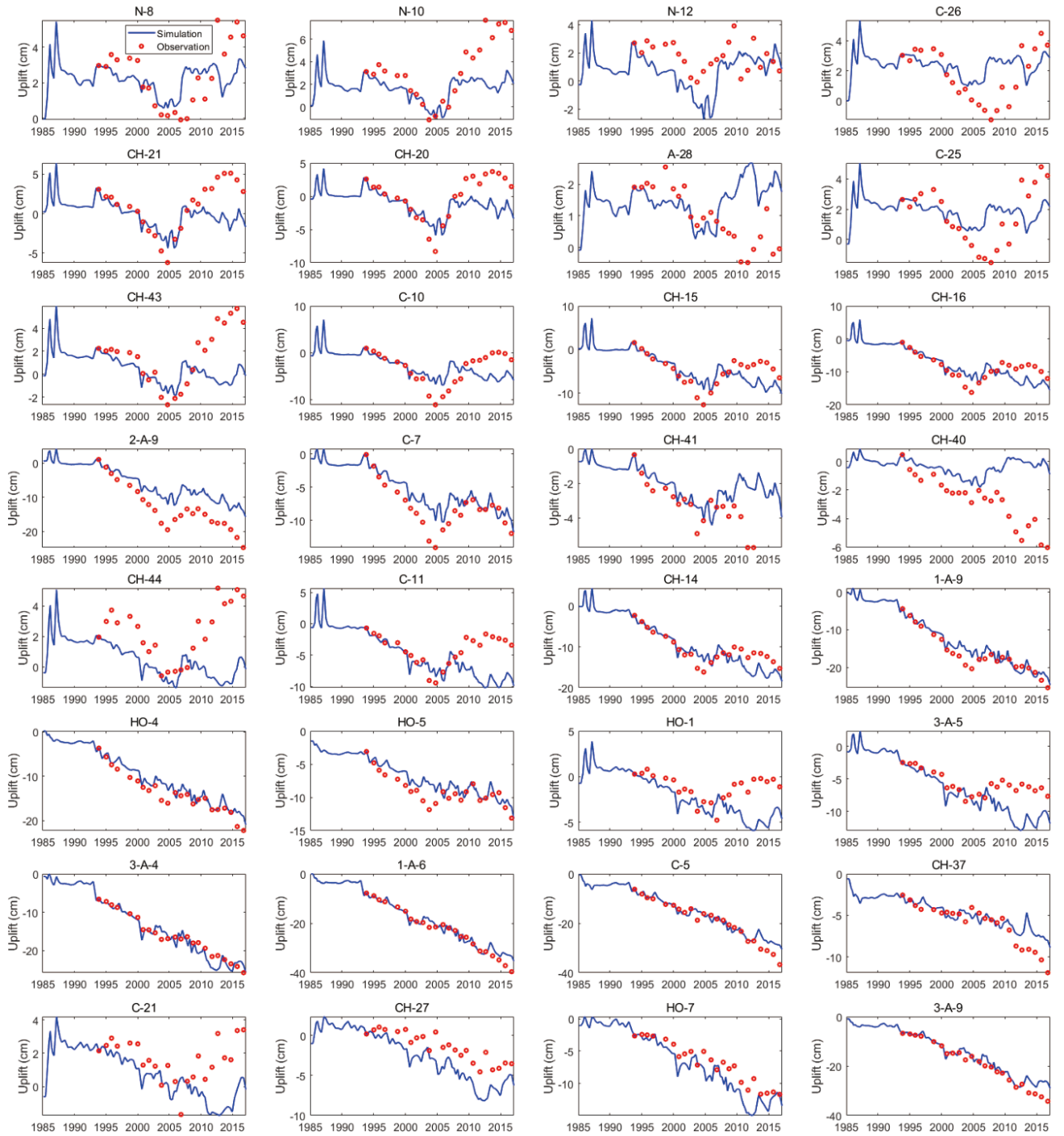
**Supplementary Fig. 11. Initial temperature distribution model of the HGF for 3D thermo-hydro-mechanical (THM) simulation.**



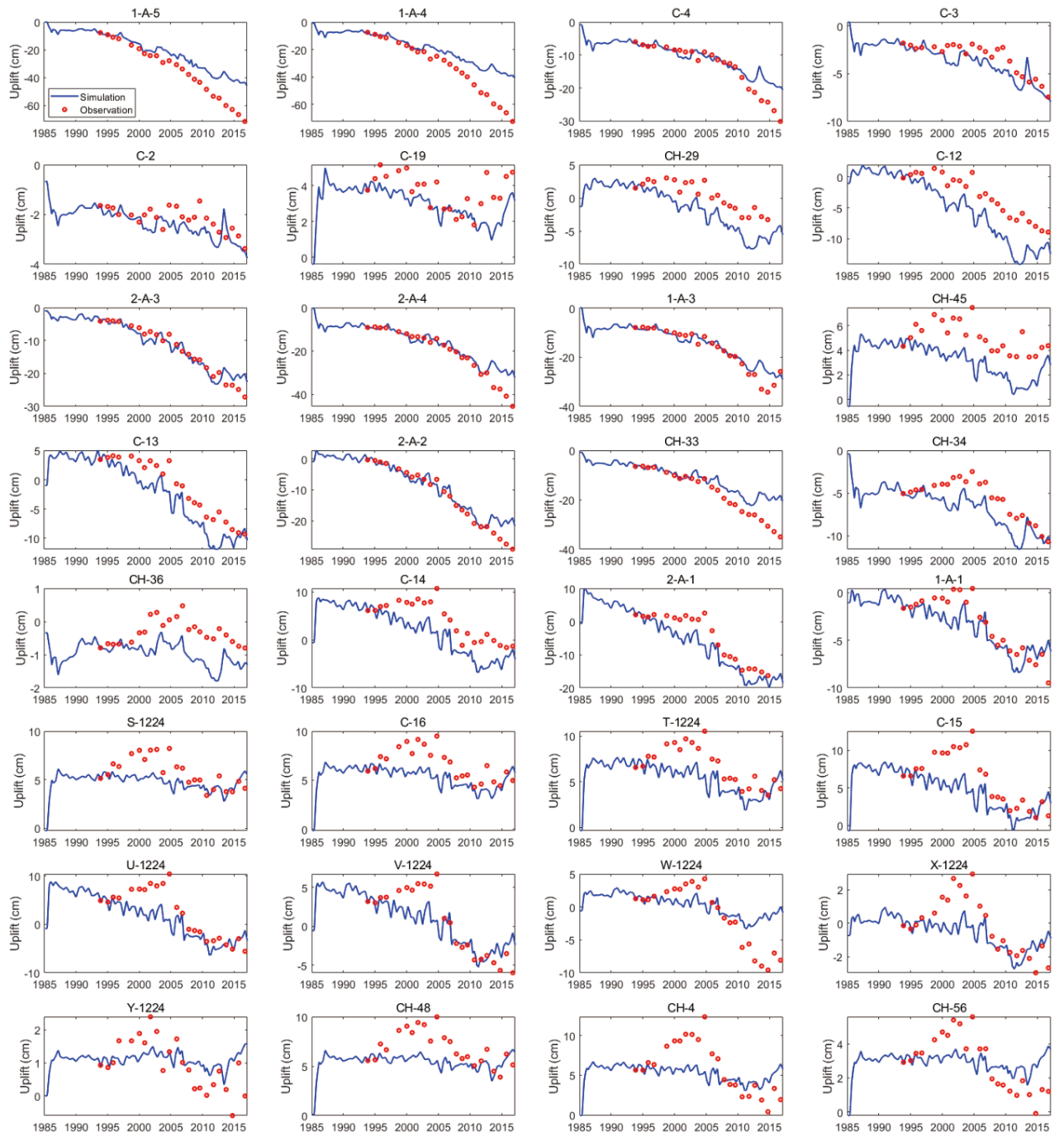
Supplementary Fig. 12. Flowchart of thermo-hydro-mechanical coupling. The arrows labeled with blue words show the effects included in our simulations.



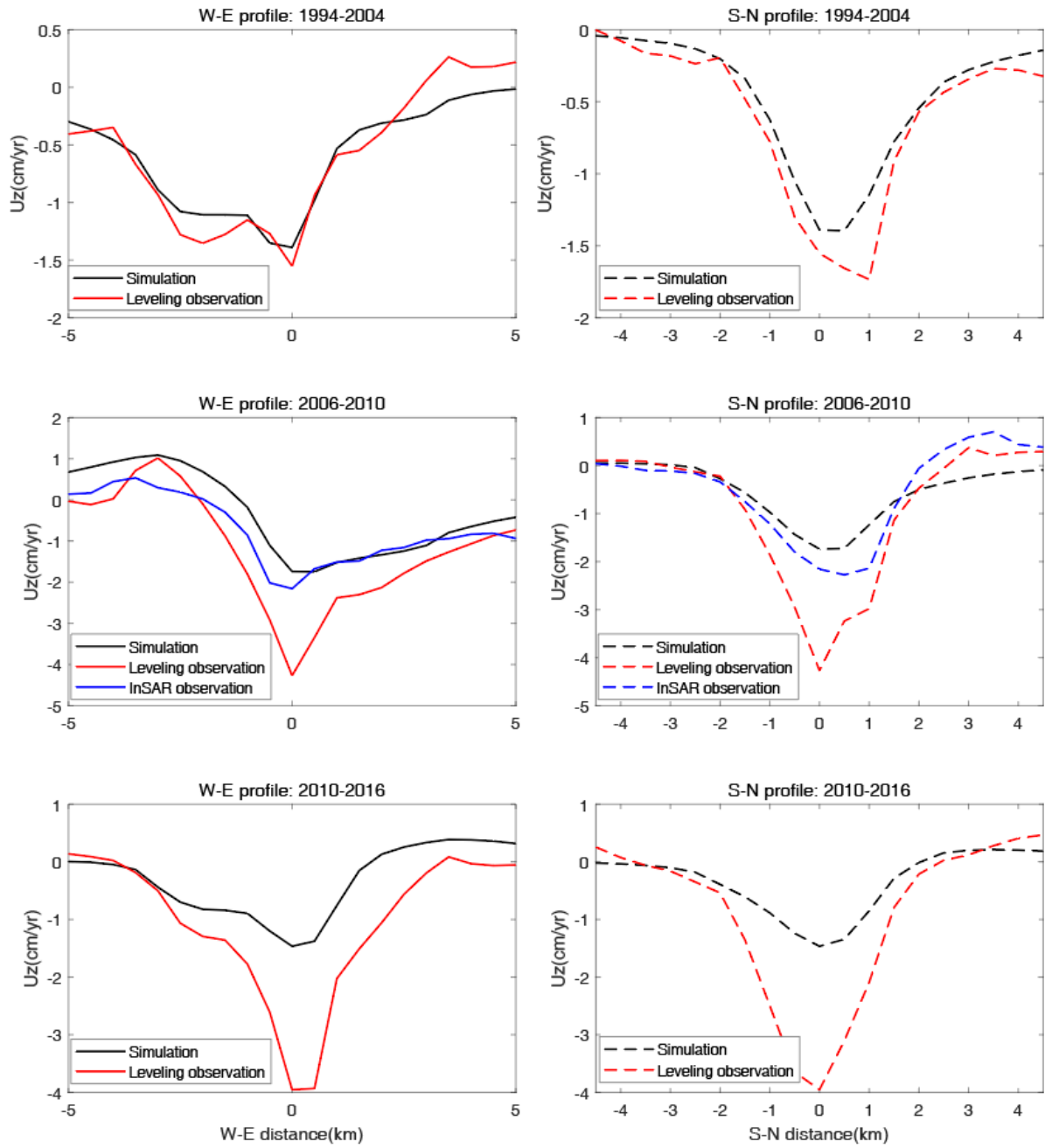
**Supplementary Fig. 13. Simulated horizontal surface displacement with the calibrated model in five time periods.** Eastward and northward motions are defined to be positive.



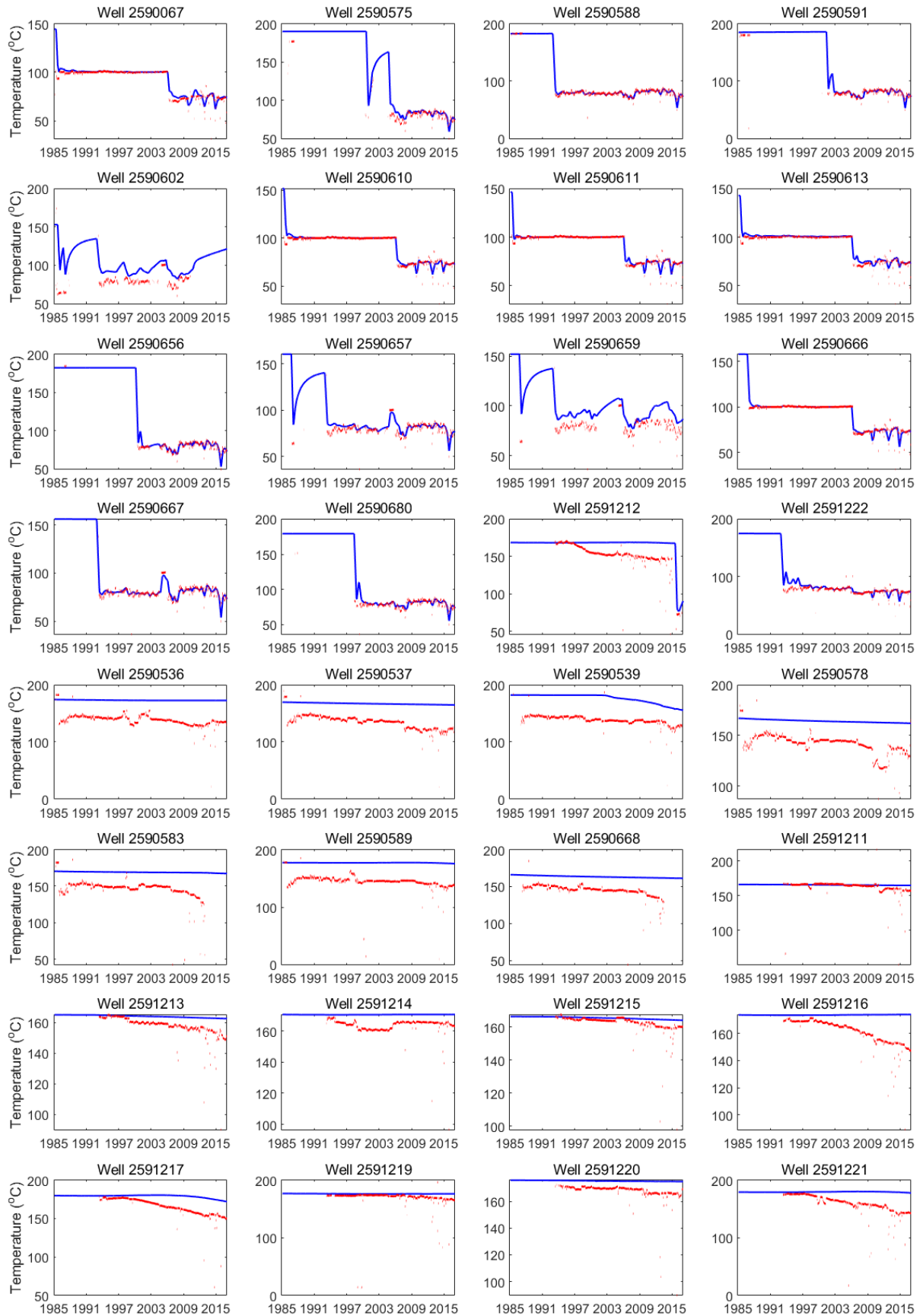
**Supplementary Fig. 14. Comparison of the vertical displacement time series observed at 64 selected benchmarks with the time series simulated by the calibrated model.**



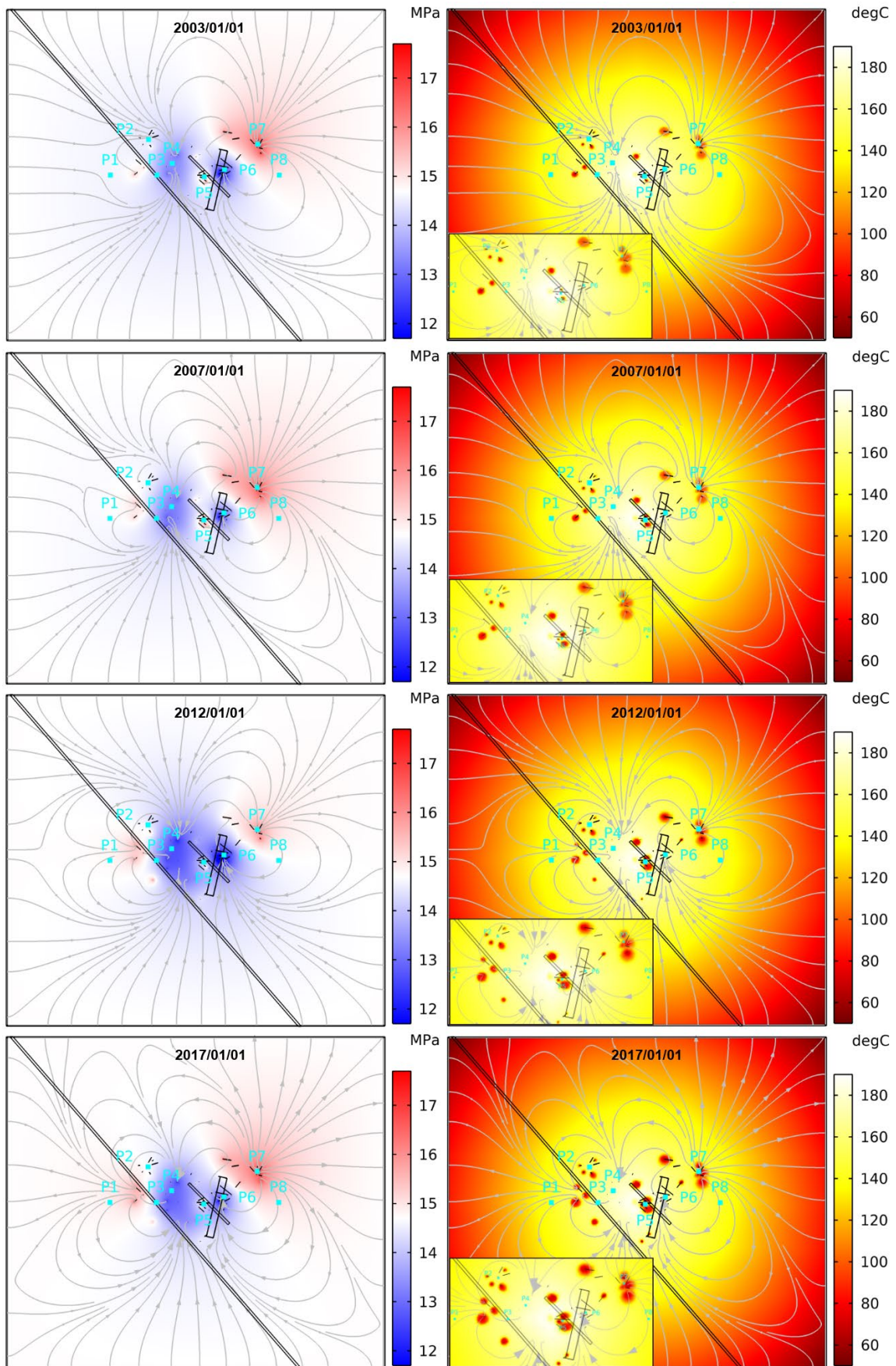
**Supplementary Fig. 14. Continued.**



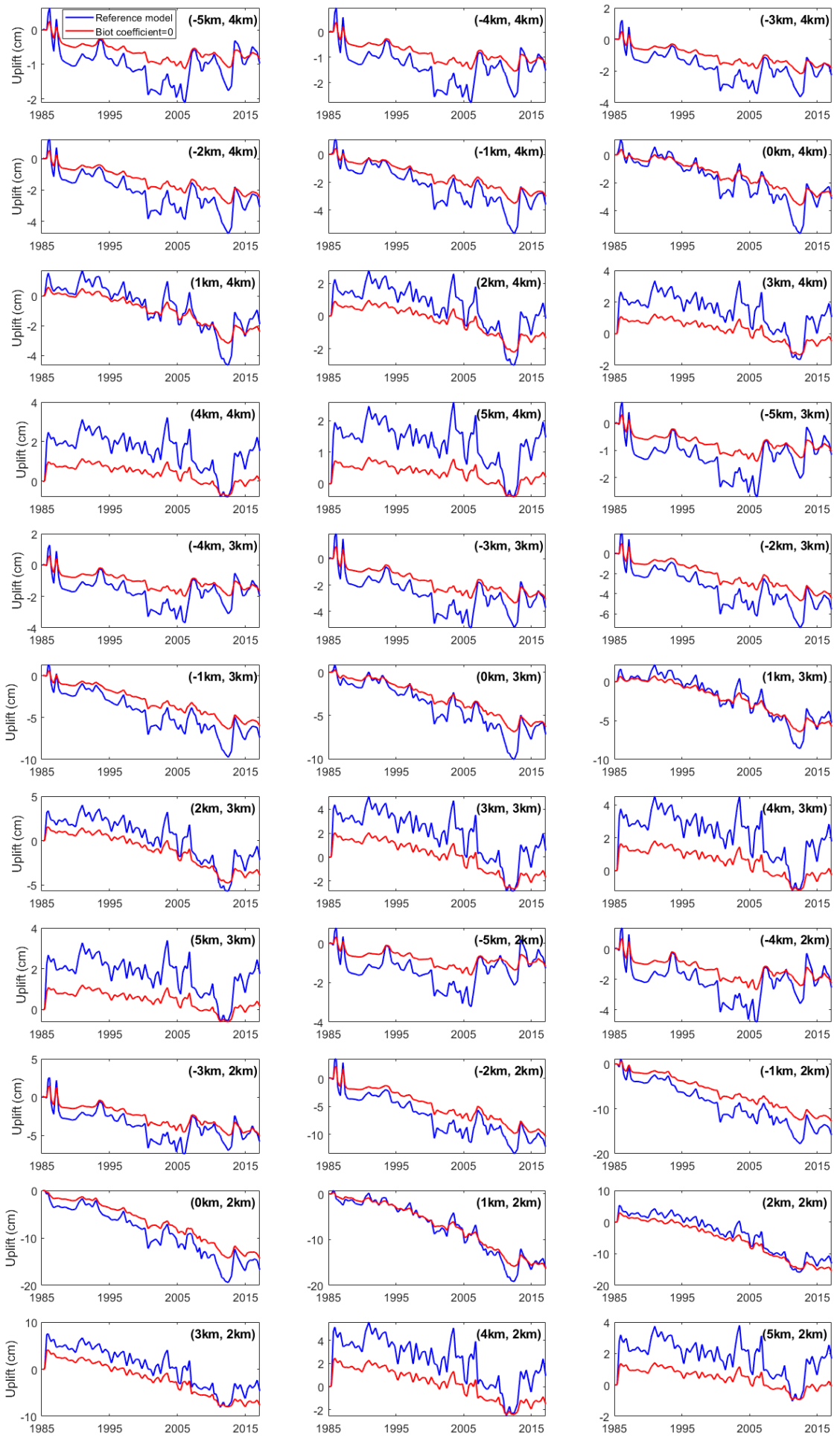
**Supplementary Fig. 15. Comparison of simulated vertical displacement with the observations along the W-E and S-N profiles. Each profile goes through the center of the HGF.**



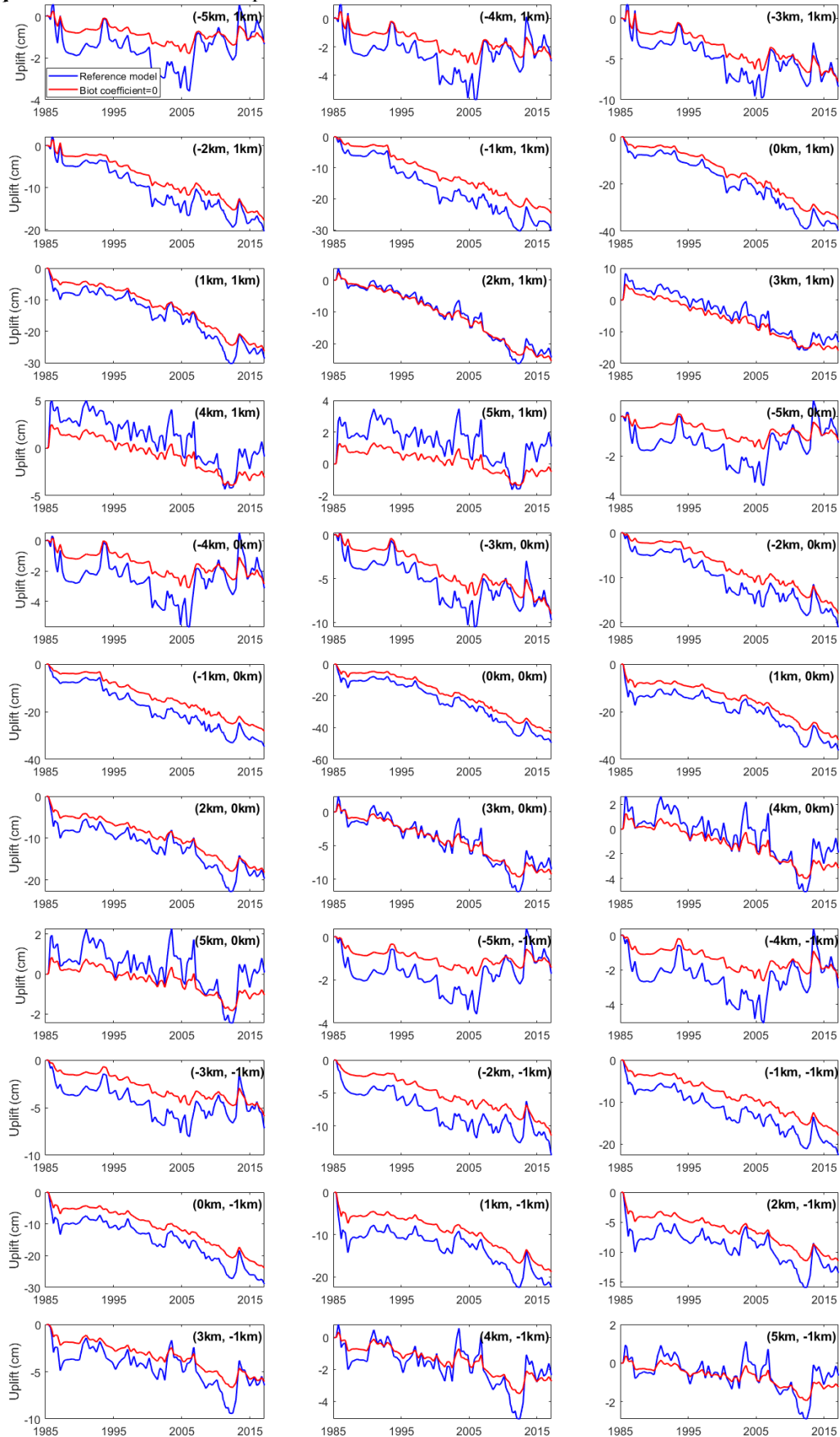
**Supplementary Fig. 16. Comparison of simulated temperature variations with the records of 32 selected wells. Red points: reported fluid temperature; blue curves: simulated well temperature with the calibrated model.**



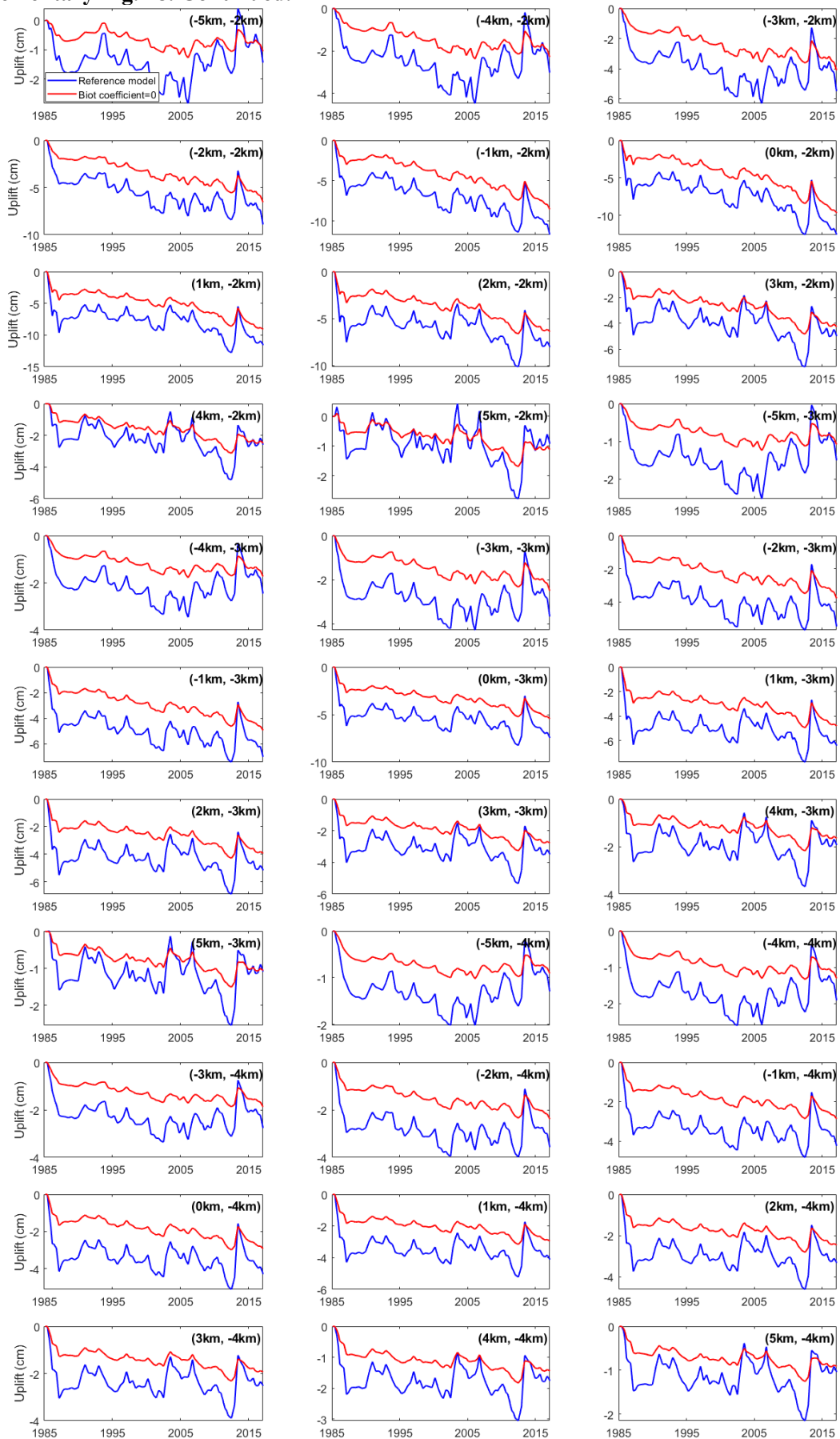
**Supplementary Fig. 17. Simulated pressure and temperature distribution with the calibrated model at the bottom of the upper reservoir layer (depth=1.5 km). Gray curves and arrows showing the movement of fluid.**



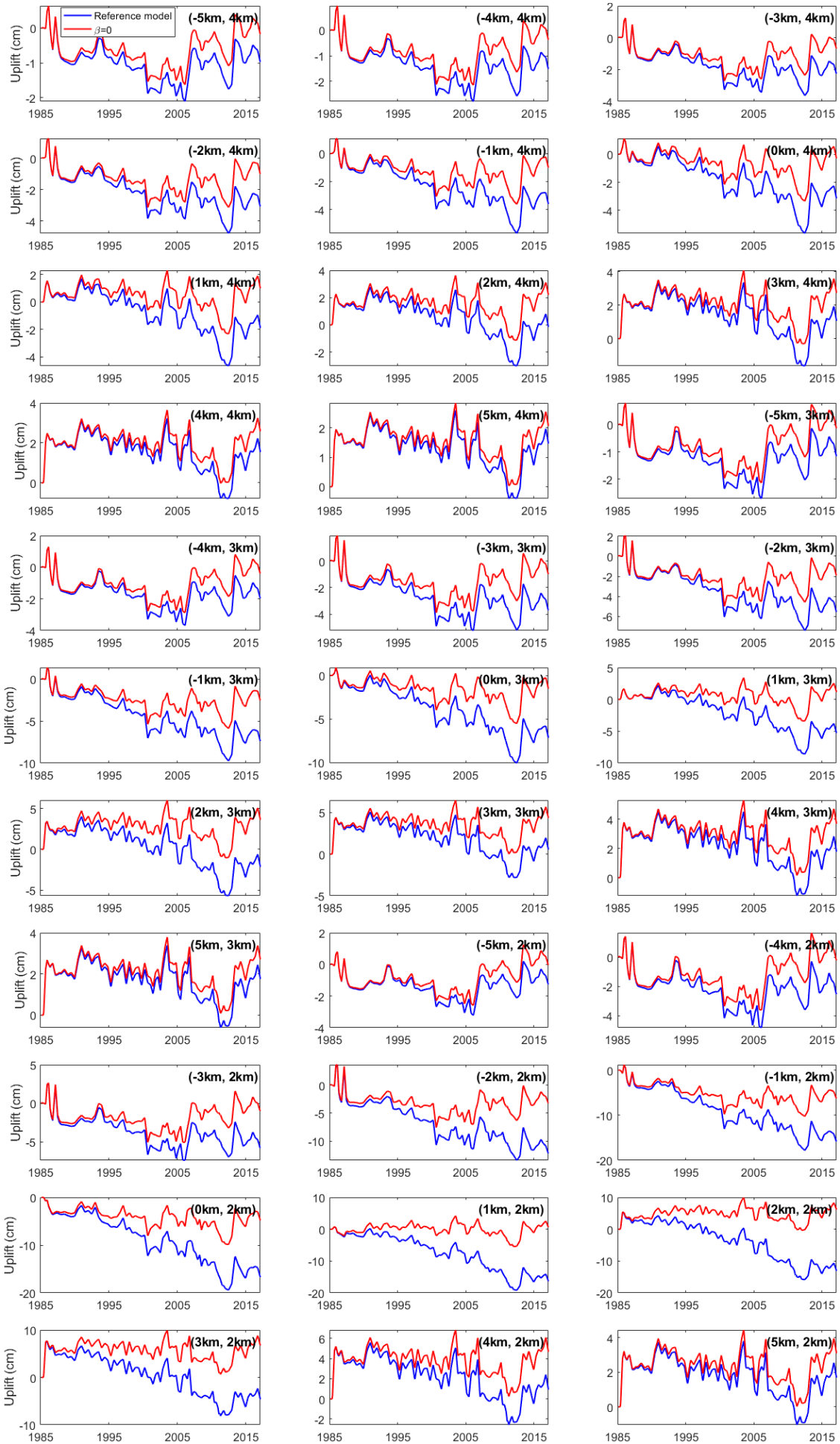
**Supplementary Fig. 18. Vertical surface displacement at 99 points simulated with the calibrated (reference) model and the model with the Biot coefficients of the two reservoirs and the feeder fault equal to 0. Locations of the points relative to the center of the model are labeled within each panel.**



Supplementary Fig. 18. Continued.

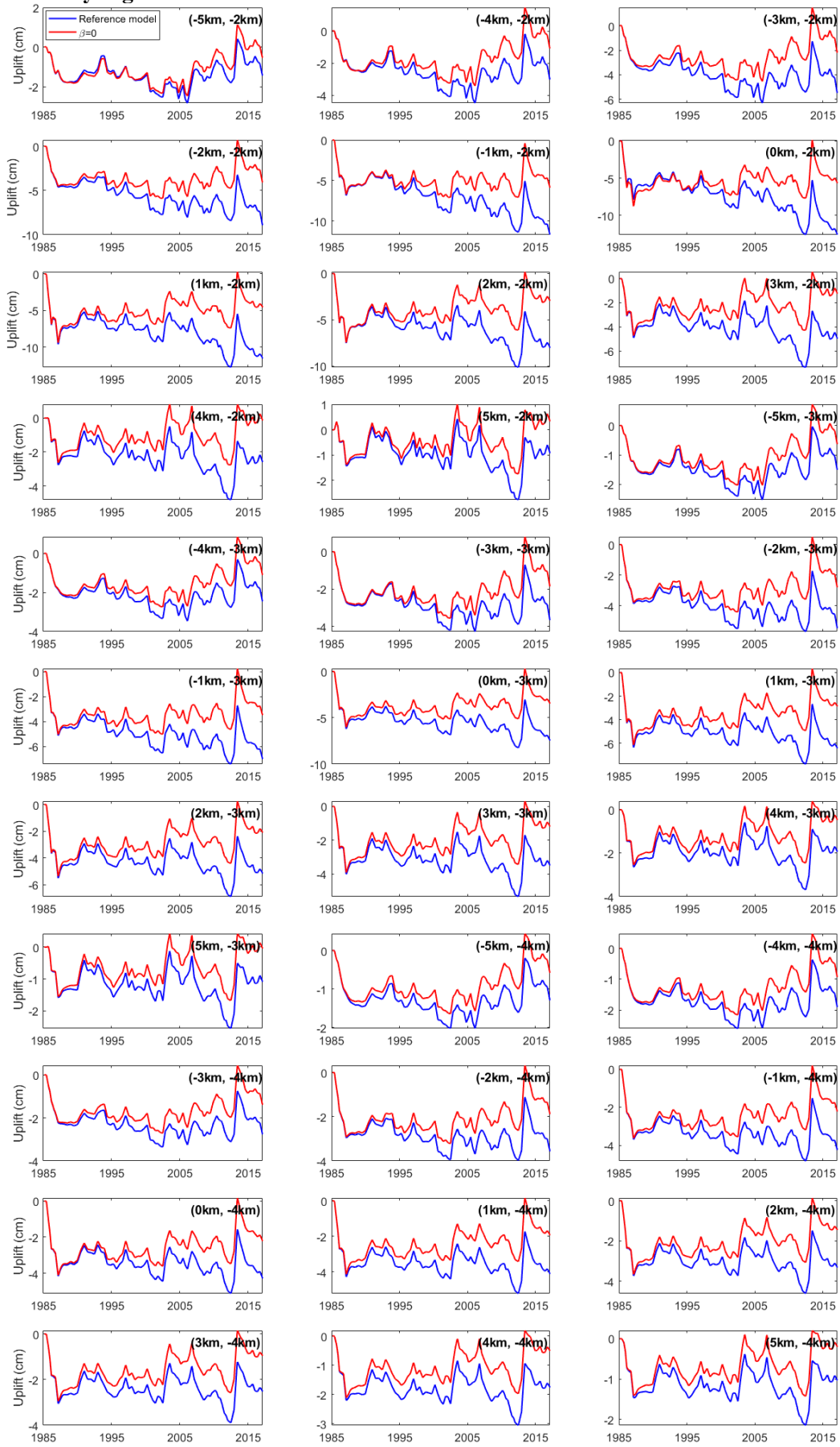


Supplementary Fig. 18. Continued.

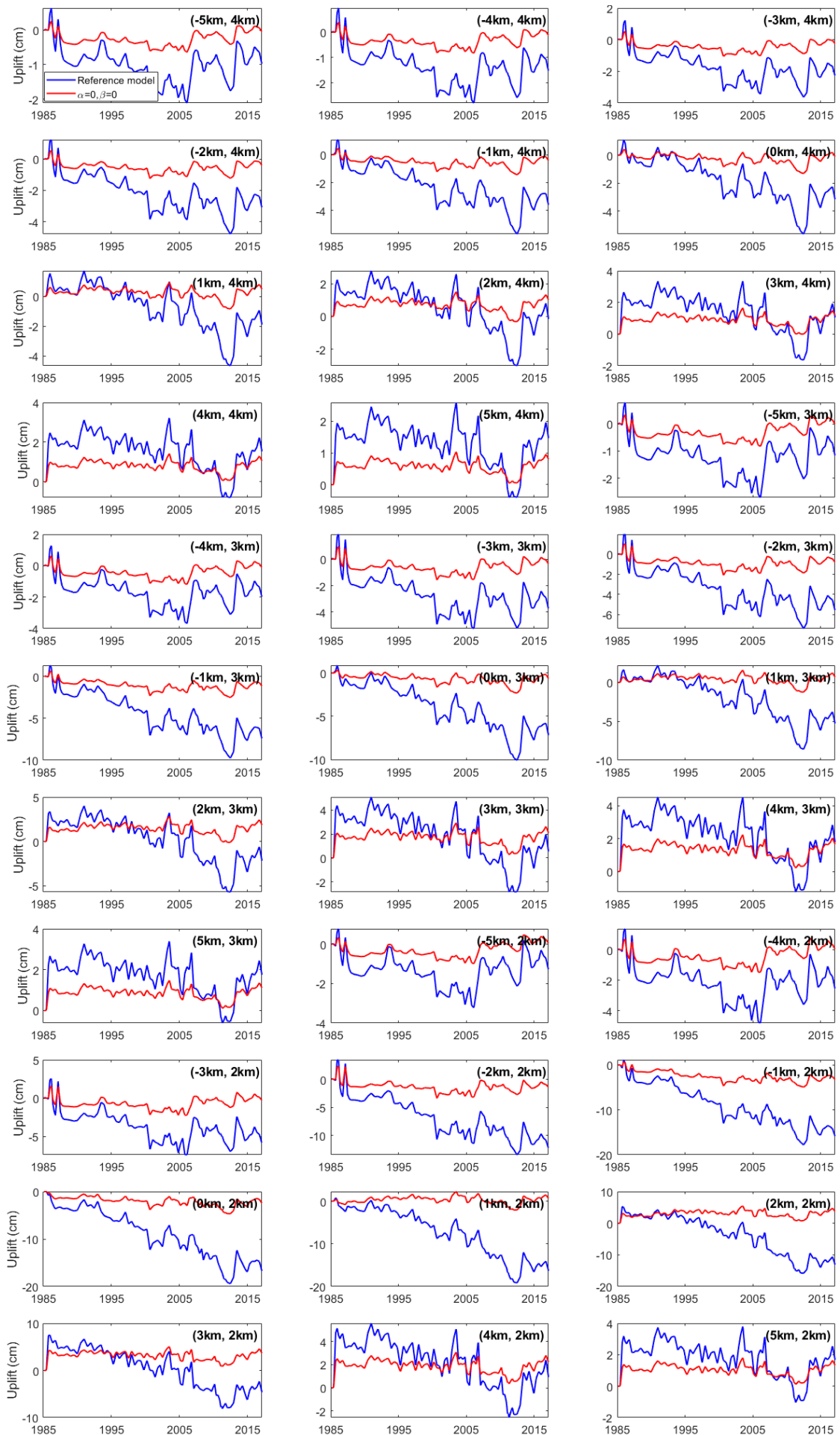




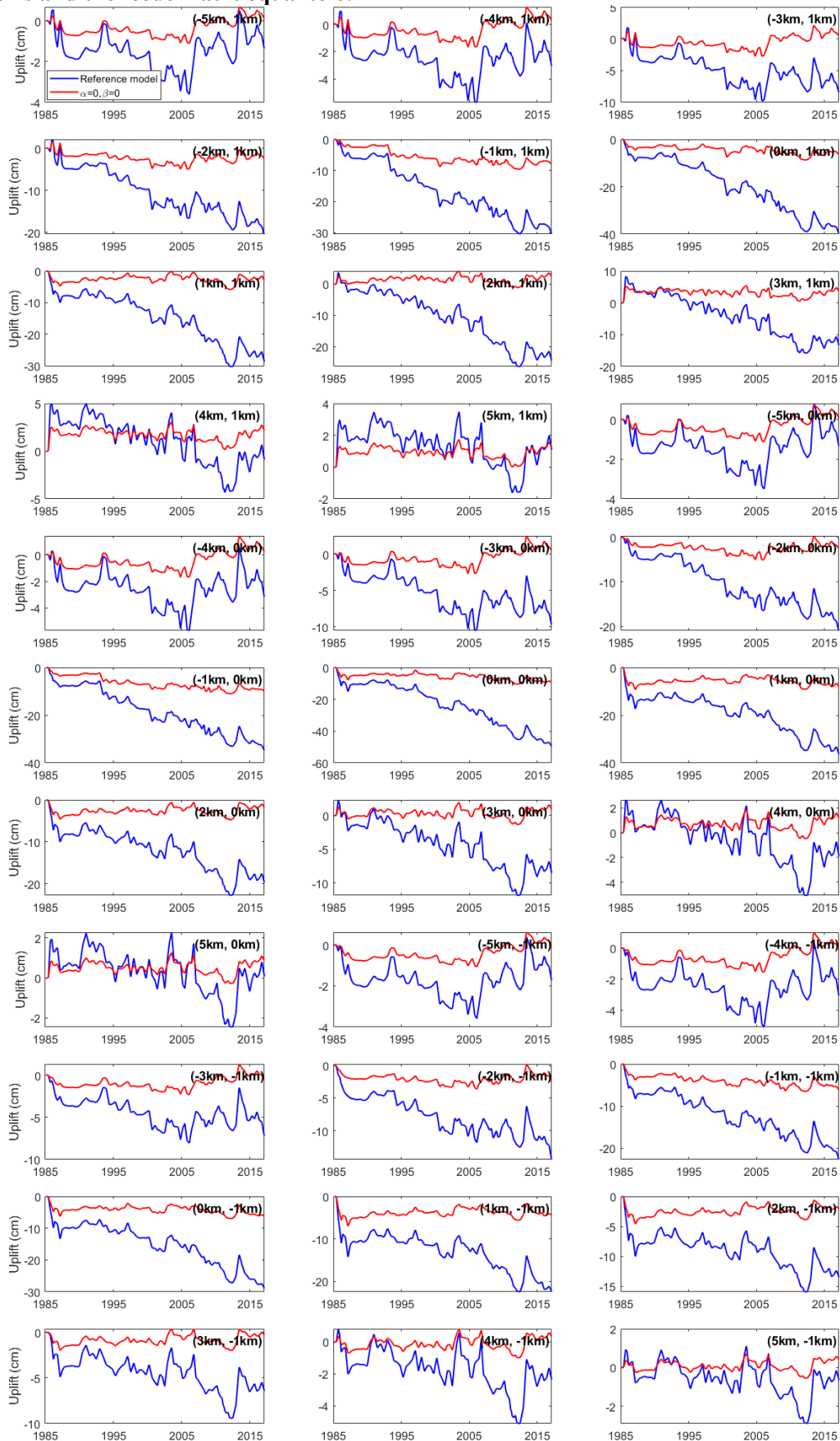
Supplementary Fig. 19. Continued.



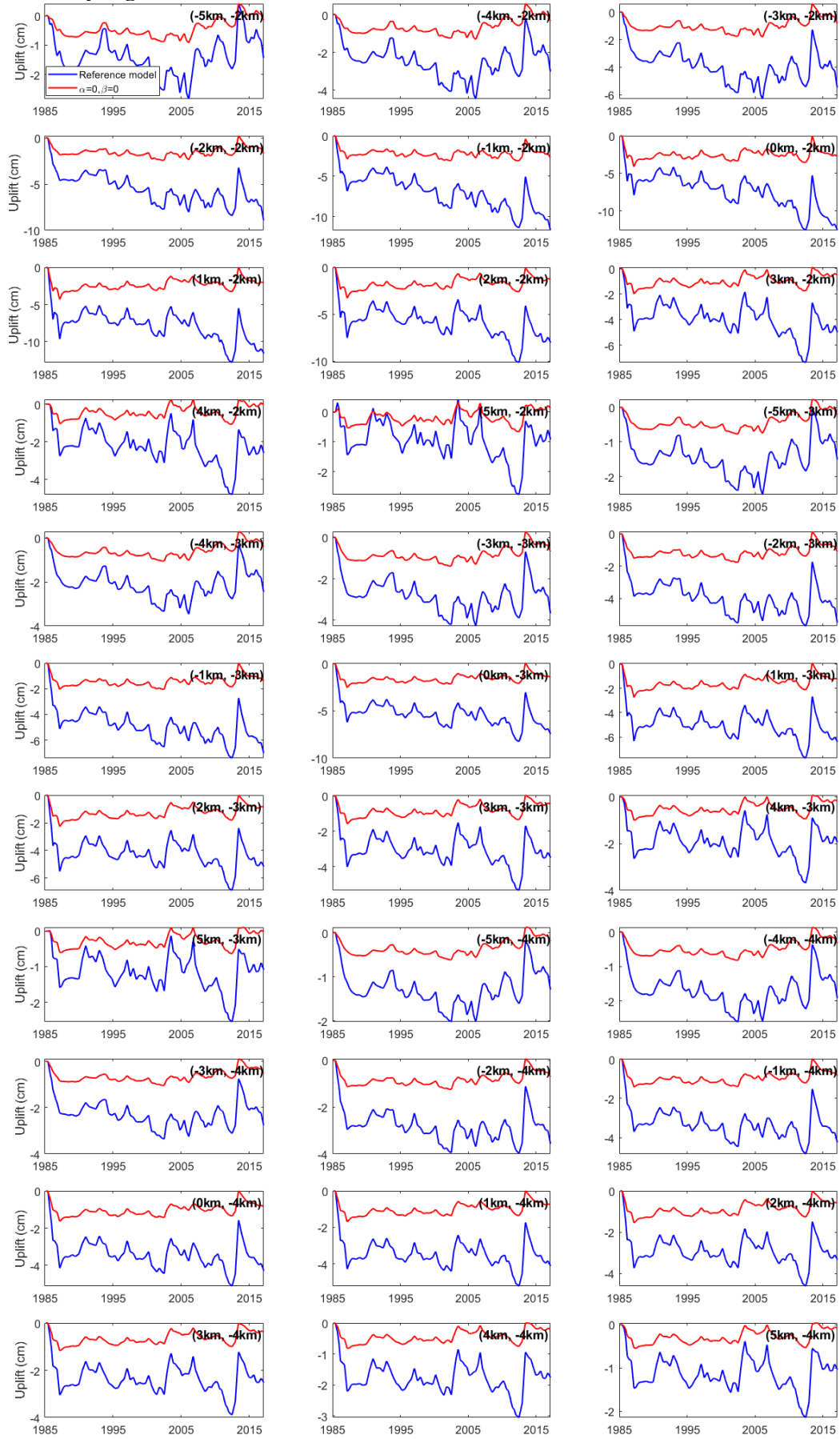
Supplementary Fig. 19. Continued.



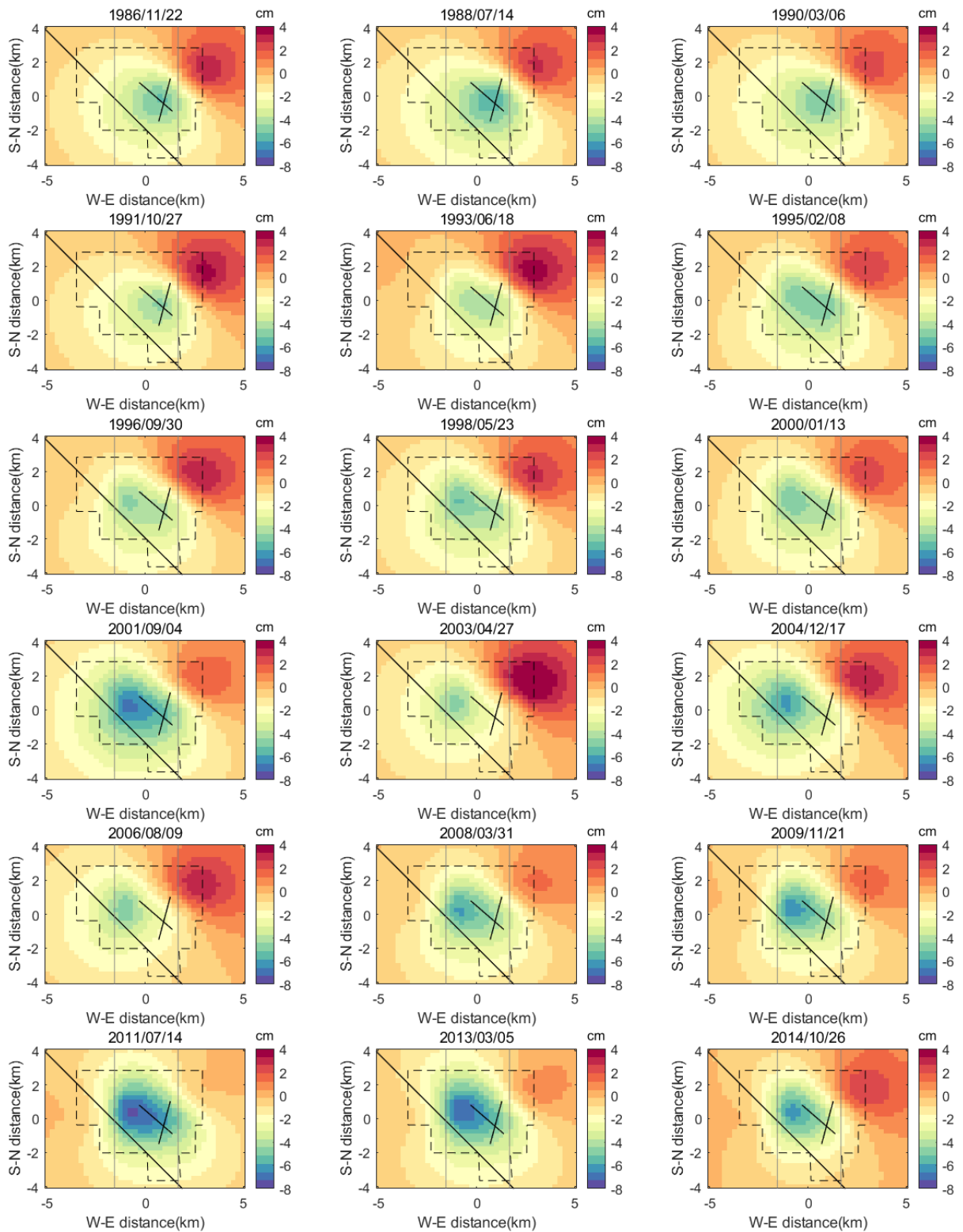
**Supplementary Fig. 20. Vertical surface displacement at 99 points simulated with the calibrated (reference) model and the model with the Biot ( $\alpha$ ) and thermal expansion coefficients of the two reservoirs and the feeder fault equal to 0.**



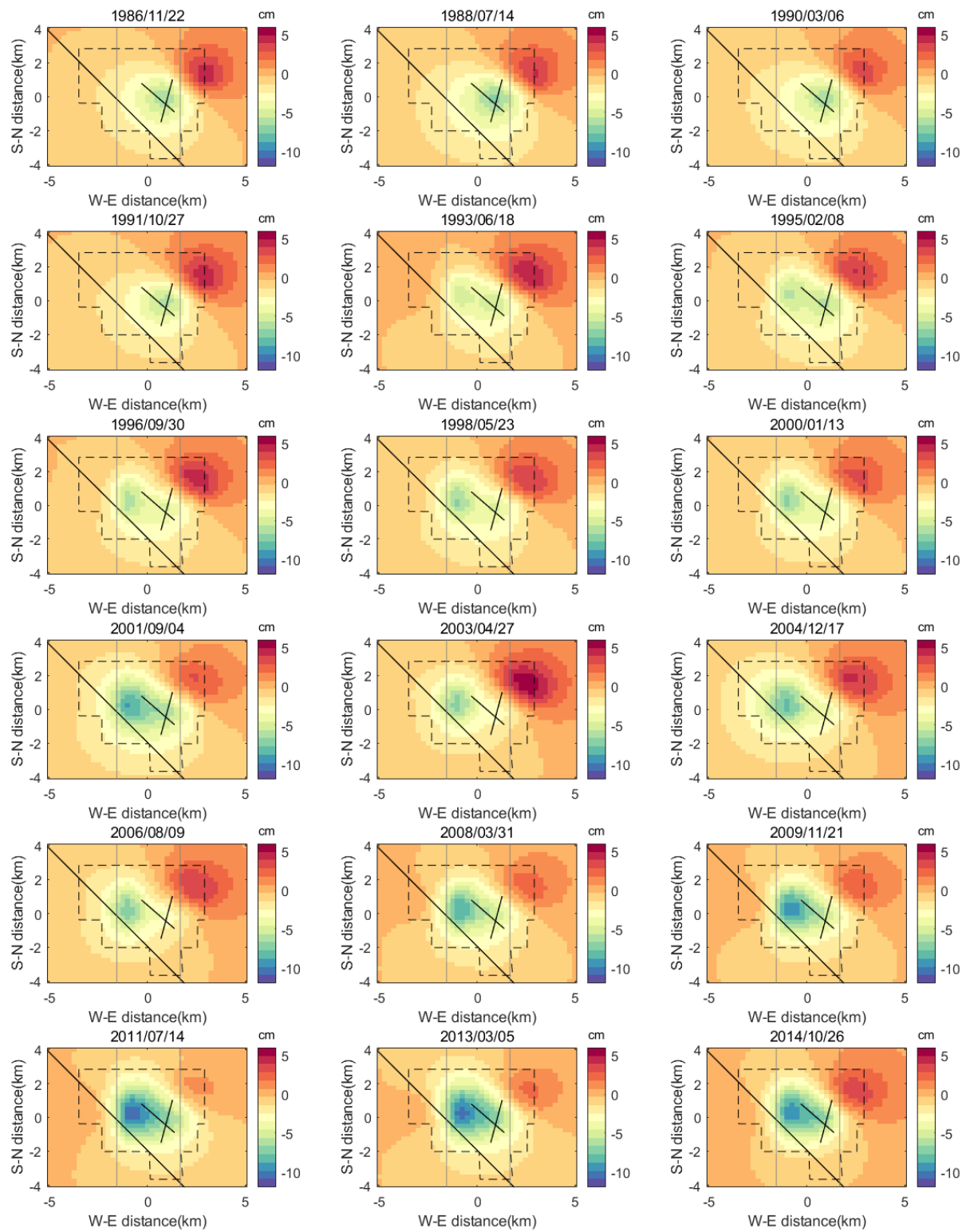
Supplementary Fig. 20. Continued.



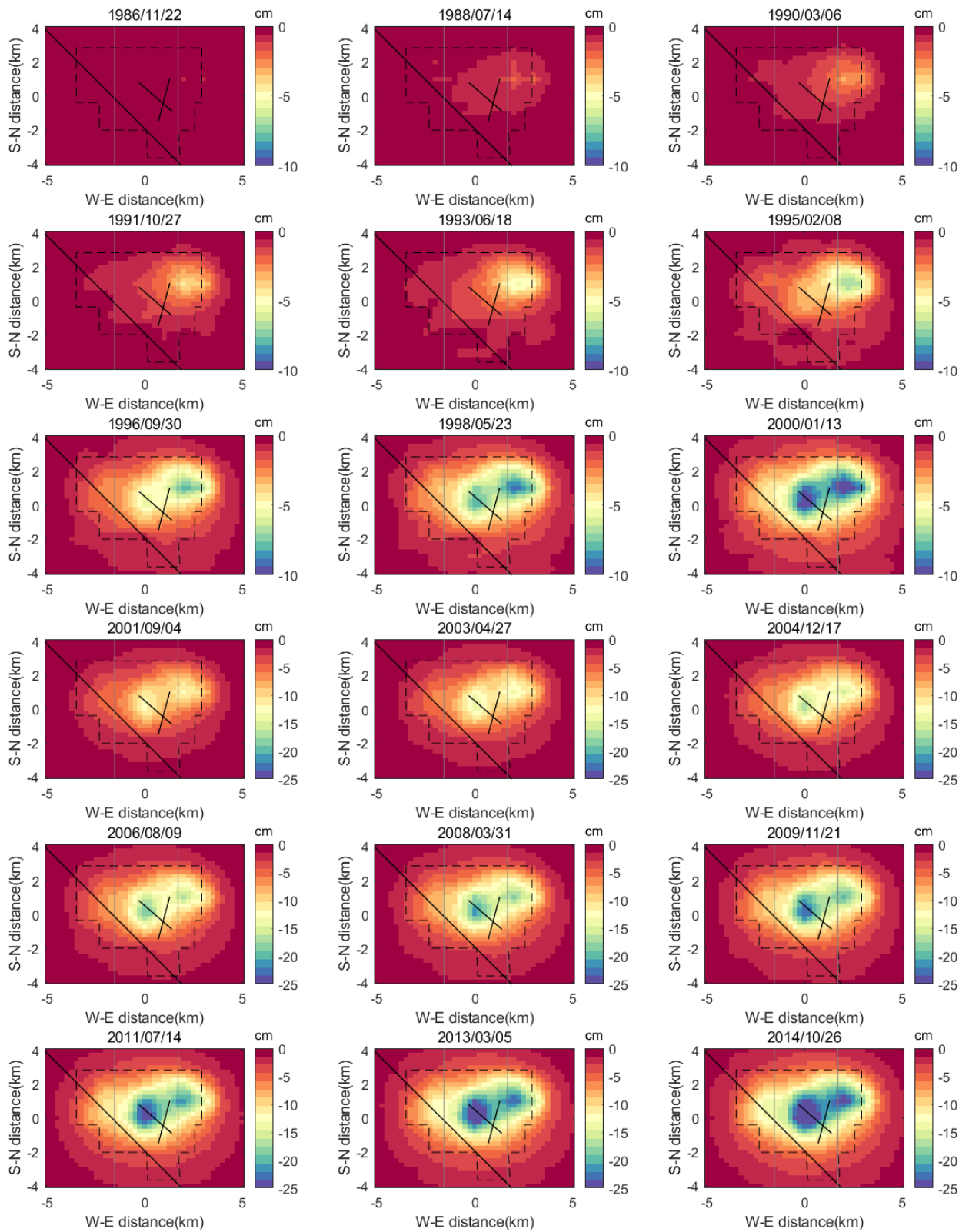
Supplementary Fig. 20. Continued.



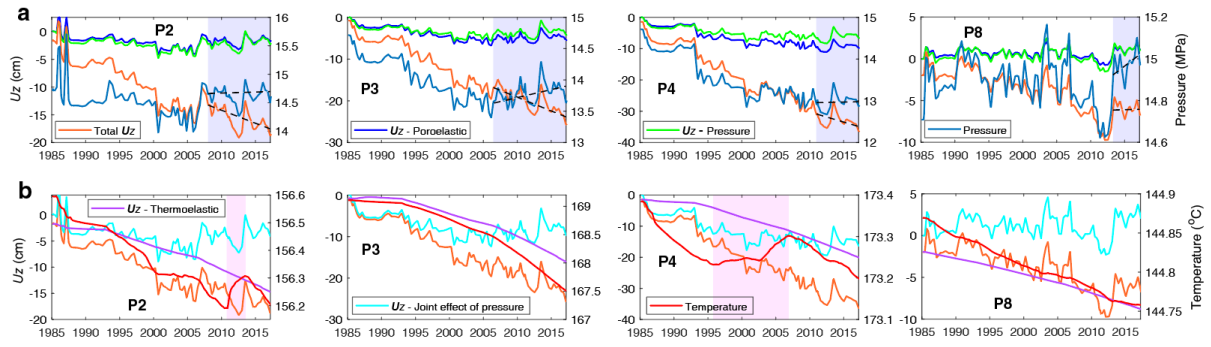
**Supplementary Fig. 21. Vertical surface displacement caused by pressure variation at different time nodes.**



**Supplementary Fig. 22. Vertical surface displacement caused by poroelastic effects of expansion and contraction at different time nodes.**



**Supplementary Fig. 23. Vertical surface displacement caused by thermoelastic effect of contraction at different time nodes.** As the thermal effect increases with time, we use two color scales for two time periods of 1985-2000 and 2001-2014.



**Supplementary Fig. 24. Temporal evolution of thermo-poro-elastic effects at four probe points (see Figs. 7 and 8 in the main text for their locations). a** Temporal evolution of the effects of pressure fluctuation and poroelastic response at four probe points. Shaded regions mark the time periods with contrary trends of cumulative vertical displacement and pressure changes (marked with black dashed lines). **b** Temporal evolution of the thermal contraction effect at four probe points. Shaded regions show the time periods with opposing trends in cumulative vertical displacement and temperature.

## Supplementary tables

**Supplementary Table 1. 69 operation wells of the HGF.**

Well ID	Injection time period	Extraction time period	Vertical well	Depth ranges of open-hole section (m)	Zone
2590007	1993/06/01-2017/05/31		YES	649.83-1072.9; 1190.55-1507.24	West
2590039	1993/06/01-2017/05/31		YES	615.09-1584.96	Central
2590067	1985/05/01-2017/05/31		YES	617.3-1173.3	East
2590536		1985/04/01-2017/05/31	NO	1350.3-2280.5	Central
2590537		1985/04/01-2017/05/31	NO	784.9-1334.4	Central
2590538		1985/04/01-2013/08/10	NO	1282-1889.8	Central
2590539		1985/10/01-2017/05/10	NO	777.2-1103.1	Central
2590540		1985/05/01-2016/11/30	NO	865.6-1037.5; 2440.2-3211.4	Central
2590574		1985/04/01-2017/04/09	NO	1325.9-2211.9	Central
2590575	2000/09/01-2017/05/31	1985/04/01-1989/03/01; 2001/10/01-2002/02/10	NO	2442.06-3269.59	Central
2590578		1985/05/01-2017/05/31	YES	885.1-1495.5	Central
2590582		1985/04/01-2017/05/31	NO	1050.3-1659.3	Central
2590583		1985/05/01-2013/03/15	NO	799.5-1528.0	Central
2590584	2000/08/03-2017/05/31	1985/05/01-1989/03/01	NO	1213.1-2057.7	Central
2590585	2005/04/01-2017/05/31	1985/04/01-1989/03/01	NO	854-1400.1	Central
2590587	2001/01/01-2015/04/19	1985/06/01-1989/02/01	NO	1320.6-1994.1	Central
2590588	1993/06/01-2017/05/31	1985/04/01-1989/03/01	NO	886.3-1462.8	Central
2590589		1985/05/01-2017/05/31	NO	1266.4-2081.5	Central
2590590	1985/06/01-2016/11/30		NO	610.5-906.8; 1219.2-3028	East
2590591	2000/09/01-2017/05/31	1985/06/01-1989/03/01	NO	1302.6-1918.4	Central
2590592	2006/09/01-2017/05/31	1985/06/01-1989/03/01	NO	727.4-1528.4	Central
2590600	1985/05/01-2017/05/31		NO	622.5-1349.3	East
2590601	1985/06/01-2017/05/31		NO	1236.5-1950.8	East
2590602	1985/05/01-2010/04/05		NO	654.5-1412.2	West
2590603	1985/04/01-2017/05/31		NO	1255.1-2006.9	West
2590610	1985/06/01-2017/05/31		NO	1257.8-2011.8	East
2590611	1985/06/01-2017/05/31		NO	635.3-1307.2	East

2590612	1985/06/01-2017/05/31		NO	1257.8-1895.9	East
2590613	1985/06/01-2017/05/31		NO	642-1390.8	East
2590614	1985/04/01-2017/05/31		NO	610.6-1336.5	West
2590615	1985/06/01-2017/05/31		NO	1255.1-2006.9	West
2590616	1985/06/01-2009/06/05		NO	625.2-1395.7	West
2590656	2000/09/01-2017/05/31	1987/02/01-1989/03/01	NO	2154.94-2598.42	Central
2590657	1987/01/01-2017/05/30		NO	1261.87-2031.49	West
2590659	1986/12/01-2017/01/25		NO	1269.19-2069.59	West
2590664	2000/08/01-2017/05/31		NO	1973.58-2741.68	Central
2590666	1987/03/01-2017/05/31		NO	1154.58-1854.71	East
2590667	1989/03/01-2017/05/31		NO	1158.24-1696.21	West
2590668		1987/06/01-2013/11/01	NO	694.6-1533.8	Central
2590680	1998/08/01-2017/05/31	1987/08/01-1988/01/18	NO	2202.5-2940	Central
2591211		1993/06/01-2017/05/31	YES	751-1211	Central
2591212	2016/01/01-2017/01/31	1993/06/01-2015/04/20	NO	749.6-1230	Central
2591213		1993/06/01-2017/05/31	YES	745.6-1226.3	Central
2591214		1993/06/01-2017/05/31	YES	740.5-1825.7	Central
2591215		1993/06/01-2017/05/31	YES	607.7-1228	Central
2591216		1993/06/01-2017/05/31	YES	725-1220	Central
2591217		1993/06/01-2017/05/31	YES	647-1231	Central
2591218		1993/06/01-2017/05/31	YES	795-1843	Central
2591219		1993/06/01-2017/05/29	YES	597.4-1220	Central
2591220		1993/06/01-2017/05/31	YES	771-1211.8	Central
2591221		1993/06/01-2017/05/31	YES	677.5-1236	Central
2591222	1993/06/01-2017/05/31		YES	701.3-1371	Central
2591224	1993/06/01-2017/05/31		YES	785.7-1370	Central
2591229	1993/05/01-2017/05/31		NO	754.6-1295.4	East
2591265		2006/01/01-2017/05/31	YES	773.5-1689.6	Central
2591424	2006/06/01-2017/05/29		NO	827.53-2007.11	East
2591425	2008/04/01-2016/12/30		YES	1302.11-1876	Central
2591430		2007/01/01-2017/05/31	YES	548.6-754.7	Central
2591431	2006/10/01-2017/05/31		NO	643.74-1935.18	West

2591432	2008/04/01-2017/05/31		YES	775.41-1823.31	Central
2591435		2008/04/01-2017/05/31	YES	860.5-1212.5	Central
2591439	2008/04/01-2017/05/31		NO	964.08-1774.55	Central
2591441		2008/04/01-2009/07/05	NO	844-924.5	Central
2591478		2009/07/01-2017/05/31	YES	705.6-1529.2	Central
2591489		2011/01/01-2017/05/31	YES	711.7-1467.9	Central
2591497		2011/06/01-2017/05/31	YES	569.4-991.2	Central
2591506		2013/05/01-2017/05/31	YES	581.3-1004.9	Central
2591507		2013/05/01-2017/05/31	YES	587-1195	Central
2591511		2016/01/01-2017/05/18	NO	564.8-1081.1	Central

**Supplementary Table 2. Mechanical, hydraulic and thermophysical parameters in the Heber geothermal reservoir model**

Formation	Thickness (km)	Density (kg/m <sup>3</sup> )	Young's modulus (GPa)	Biot coefficient		Poisson's ratio	Porosity (%)	Permeability (10 <sup>-15</sup> m <sup>2</sup> )		Specific heat (J/(kg·°C)) <sup>c</sup>	Thermal conductivity (W/(m·°C))	Thermal expansion coefficient (°C <sup>-1</sup> )
				I <sup>a</sup>	II <sup>b</sup>			Horizontal	Vertical			
Caprock	0.55	1719	0.31	0.97	0.98	0.49	3	0.28	0.28	1000	1	1E-5
Upper reservoir	1.10	2045	5.24	<b>0.85</b>	0.91	0.42	<b>18</b>	<b>20</b>	<b>20</b>	<b>1000</b>	<b>2→3</b>	<b>1E-5</b> <b>→1.3E-5</b>
Lower reservoir	1.50	2362	27.87	<b>0.67</b>	0.76	0.28	<b>18</b>	<b>20→10</b>	<b>20→10</b>	<b>1000</b>	<b>2→3</b>	<b>1E-5</b> <b>→1.3E-5</b>
Basal layer	1.15	2565	60.33	0.57	0.44	0.22	10	5	0.28	1000	2	1E-5
Basement	2.70	2622	69.15	0.56	0.39	0.23	5	1	0.28	1000	1	1E-5
Feeder fault	<b>0.30</b>	2500	<b>10</b>	0.70	0.85	<b>0.3</b>	<b>20</b>	<b>20</b>	<b>20</b>	<b>1000</b>	<b>2</b>	<b>1E-5</b>
Boundary fault	<b>0.10</b>	2500	10	0.64	0.85	0.3	<b>5</b>	<b>5</b>	<b>5</b>	<b>1000</b>	<b>1</b>	1E-5
Subsidiary fault	<b>0.10</b>	2500	10	0.70	0.85	0.3	<b>20</b>	<b>20</b>	<b>20</b>	<b>1000</b>	<b>1</b>	1E-5

<sup>a</sup>The Biot values are calculated with the equation:  $\alpha = (1 + \nu + 2\phi(1 - 2\nu))/(3(1 - \nu))$  (Zimmerman *et al.*, 1986).  $\nu$  and  $\phi$  are the Poisson's ratio and porosity of rock within each formation.

<sup>b</sup>The Biot values are calculated with the equation:  $\alpha = 1 - K/K'_s$  (Wang, 2000), where the drained bulk modulus  $K$  is equal to  $E/[3(1 - 2\nu)]$ .  $K'_s$  is the unjacketed bulk modulus, often called the solid-grain modulus, and is assumed to be 100 GPa.

<sup>c</sup>The value of specific heat varies from 800 J/(kg·°C) to 1200 J/(kg·°C) with the temperature increasing from 50°C to 200°C for different rocks (Roberston, 1988).

Yellow cells mark the parameters considered in model calibration. The cells with one value indicate that the initial parameter setting is optimal. For the cells with two values, the values at the start and end of each arrow correspond to the initial parameter setting and the calibration result, respectively.

**Supplementary Table 3. Misfits between simulation results with different model sizes and observations.**

Model size			RMS misfit		
Length (km)	Width (km)	Height (km)	Leveling (cm)	InSAR (cm)	Temperature (°C)
15	13	7	3.99	2.44	21.51
15	13	8	3.59	2.77	21.84
16	14	8	2.90	2.86	21.55
17	15	8	2.96	2.63	21.42
17	15	9	3.26	2.90	21.69

**Supplementary Table 4. Misfits of model predictions with different reservoir porosities to surface displacement and temperature observations. Orange and green values correspond to the first and second rounds of model calibration, respectively.**

**I. RMS misfits to Leveling observations (cm)**

Porosity		Upper reservoir			
		14%	16%	18%	20%
Lower reservoir	14%	3.17	3.33	3.13	3.38
	16%	3.30	2.98 2.48	3.21 2.51	3.27 3.28
	18%	3.72	3.10 2.70	2.90 2.39	3.43 3.35
	20%	3.51	3.44 3.18	3.02 2.80	3.56 2.80

**II. RMS misfits to InSAR observations (cm)**

Porosity		Upper reservoir			
		14%	16%	18%	20%
Lower reservoir	14%	2.62	2.71	2.38	2.54
	16%	2.48	2.69 2.61	2.69 2.48	2.62 5.04
	18%	3.47	2.68 3.43	2.86 2.68	2.52 3.02
	20%	2.87	3.04 2.63	2.68 2.81	2.63 2.47

**III. Weighted RMS misfits of deformation<sup>a</sup>(cm)**

Porosity		Upper reservoir			
		14%	16%	18%	20%
Lower reservoir	14%	3.06	3.21	2.98	3.21
	16%	3.14	2.92 2.51	3.11 2.50	3.14 3.63
	18%	3.67	3.02 2.85	2.89 2.45	3.25 3.28
	20%	3.38	3.36 3.07	2.95 2.80	3.37 2.73

**IV. RMS misfits to well temperature (°C)**

Porosity		Upper reservoir			
		14%	16%	18%	20%
Lower reservoir	14%	21.25	22.51	21.67	21.15
	16%	21.19	21.15 21.71	21.48 20.61	20.79 21.72
	18%	20.95	21.16 20.84	21.55 20.30	20.71 20.61
	20%	21.40	21.59 20.57	20.96 20.26	20.81 20.90

<sup>a</sup>The weighted misfits are calculated with the equation:  $0.8 \times (\text{Leveling misfits}) + 0.2 \times (\text{InSAR misfits})$

**Supplementary Table 5. Misfits of model predictions with different permeabilities of the upper reservoir to surface displacement and temperature observations. Orange and green values correspond to the first and second rounds of model calibration, respectively.**

I. RMS misfits to Leveling observations (cm)					II. RMS misfits to InSAR observations (cm)				
Permeability		Horizontal			Permeability		Horizontal		
		10 mD	20 mD	30 mD			10 mD	20 mD	30 mD
Vertical	10 mD	3.52	3.21	3.42	Vertical	10 mD	2.55	2.61	2.78
		2.87	2.47	2.81			2.98	2.50	2.52
	20 mD	3.38	2.90	3.10		20 mD	4.19	2.86	2.58
3.63		2.39	2.89	2.83	2.68		2.54		
30 mD	3.03	3.19	3.40	30 mD	2.99	2.73	2.75		
	2.91	2.44	3.11		2.78	3.46	2.87		

III. Weighted RMS misfits of deformation (cm)					IV. RMS misfits to well temperature (°C)				
Permeability		Horizontal			Permeability		Horizontal		
		10 mD	20 mD	30 mD			10 mD	20 mD	30 mD
Vertical	10 mD	3.33	3.09	3.29	Vertical	10 mD	21.23	21.09	20.93
		2.89	3.48	2.75			21.43	20.12	20.47
	20 mD	3.54	2.89	3.00		20 mD	20.60	21.55	21.26
3.47		2.45	2.82	20.86	20.30		20.63		
30 mD	3.02	3.10	3.27	30 mD	20.79	20.45	21.11		
	2.88	2.64	3.06		20.89	21.29	20.97		

**Supplementary Table 6. Misfits of model predictions with different permeabilities of the lower reservoir to surface displacement and temperature observations. Orange and green values correspond to the first and second rounds of model calibration, respectively.**

I. RMS misfits to Leveling observations (cm)					II. RMS misfits to InSAR observations (cm)				
Permeability		Horizontal			Permeability		Horizontal		
		5 mD	10 mD	20 mD			5 mD	10 mD	20 mD
Vertical	5 mD	2.88	3.62	2.91	Vertical	5 mD	2.49	3.00	2.63
		2.51	3.22	2.73			2.62	2.58	2.75
	10 mD	3.05	2.70	3.39		10 mD	3.55	2.63	2.45
2.71		2.39	2.74	4.35	2.68		2.68		
20 mD	3.17	4.09	2.90	20 mD	3.35	2.81	2.86		
	2.95	3.40	2.68		4.01	2.90	2.67		

III. Weighted RMS misfits of deformation (cm)					IV. RMS misfits to well temperature (°C)				
Permeability		Horizontal			Permeability		Horizontal		
		5 mD	10 mD	20 mD			5 mD	10 mD	20 mD
Vertical	5 mD	2.80	3.50	2.85	Vertical	5 mD	20.72	21.59	20.93
		2.53	3.09	2.73			20.69	21.48	20.93
	10 mD	3.15	2.69	3.20		10 mD	21.09	20.27	20.64
3.04		2.45	2.73	21.09	20.30		20.84		
20 mD	3.21	3.83	2.89	20 mD	21.11	21.12	21.55		
	3.16	3.30	2.68		21.25	20.95	21.85		

**Supplementary Table 7. Misfits of model predictions with different reservoir Biot coefficients to surface displacement and temperature observations. Orange and green values correspond to the first and second rounds of model calibration, respectively.**

**I. RMS misfits to Leveling observations (cm)**

Biot coefficient		Upper reservoir		
		0.7	0.85	1
Lower reservoir	0.52	2.77	2.73	2.69
	0.67	2.76	2.70	2.69
	0.82	2.76	2.72	2.69

**II. RMS misfits to InSAR observations (cm)**

Biot coefficient		Upper reservoir		
		0.7	0.85	1
Lower reservoir	0.52	2.55	2.60	2.66
	0.67	2.58	2.63	2.69
	0.82	2.61	2.67	2.73

**III. Weighted RMS misfits of deformation (cm)**

Biot coefficient		Upper reservoir		
		0.7	0.85	1
Lower reservoir	0.52	2.73	2.70	2.68
	0.67	2.72	2.69	2.69
	0.82	2.73	2.71	2.70

**IV. RMS misfits to well temperature (°C)**

Biot coefficient		Upper reservoir		
		0.7	0.85	1
Lower reservoir	0.52	20.27	20.27	20.27
	0.67	20.27	20.27	20.27
	0.82	20.27	20.27	20.27

**Supplementary Table 8. Misfits of model predictions with different thermophysical properties of the two reservoir layers to surface displacement and temperature observations. Orange and green values correspond to the first and second rounds of model calibration, respectively.**

RMS misfit	Thermal Expansion Coefficient (°C <sup>-1</sup> )						Thermal Conductivity (W/(m·°C))				
	8×10 <sup>-6</sup>	1×10 <sup>-5</sup>	1.3×10 <sup>-5</sup>	1.5×10 <sup>-5</sup>	1.8×10 <sup>-5</sup>	2×10 <sup>-5</sup>	1	2	3	4	5
Leveling (cm)	3.01	2.70 2.65	2.50 2.39	2.54 2.39	2.85 2.66	3.16	2.50	2.50	2.39	2.39	2.52
InSAR (cm)	2.62	2.63 2.63	2.68 2.68	2.73 2.73	2.81 2.81	2.87	2.73	2.68	2.68	2.73	3.18
Weighted Misfit (cm)	2.93	2.69 2.65	2.54 2.45	2.58 2.46	2.84 2.69	3.10	2.55	2.54	2.45	2.46	2.65
Temperature (°C)	20.27	20.27 20.30	20.27 20.30	20.27 20.30	20.27 20.30	20.27	20.25	20.27	20.30	20.34	20.36
RMS misfit	Specific Heat (J/(kg·°C))										
	800	900	1000	1100	1200						
Leveling (cm)	2.68	2.54	2.39	2.44	2.95						
InSAR (cm)	3.99	2.78	2.68	2.69	2.47						
Weighted Misfit (cm)	2.94	2.59	2.45	2.49	2.85						
Temperature (°C)	20.24	20.88	20.30	20.80	20.48						

**Supplementary Table 9. Misfits of model predictions with different thicknesses and properties (porosity, Young’s modulus, Poisson’s ratio, and three thermophysical parameters) of the normal-slip feeder fault to surface displacement and temperature observations.**

RMS misfit	Thickness (m)				Porosity (%)				E (GPa)			Poisson’s Ratio		
	250	300	350	400	18	20	22	24	5	10	20	0.2	0.3	0.4
Leveling (cm)	2.88	2.39	3.32	2.78	2.65	2.39	2.62	2.62	2.40	2.39	2.39	2.39	2.39	2.39
InSAR (cm)	3.05	2.68	2.48	2.78	3.89	2.68	2.52	2.55	2.69	2.68	2.68	2.68	2.68	2.68
Weighted Misfit (cm)	2.91	2.45	3.15	2.78	2.90	2.45	2.60	2.61	2.46	2.45	2.45	2.45	2.45	2.45
Temperature (°C)	21.09	20.30	20.93	20.99	20.43	20.30	20.71	20.63	20.30	20.30	20.30	20.30	20.30	20.30
RMS misfit	Thermal Expansion Coefficient (°C <sup>-1</sup> )				Thermal Conductivity (W/(m·°C))				Specific Heat (J/(kg·°C))					
	8×10 <sup>-6</sup>	1×10 <sup>-5</sup>	1.5×10 <sup>-5</sup>	2×10 <sup>-5</sup>	1	2	3	4	900	1000	1100			
Leveling (cm)	2.39	2.39	2.39	2.38	2.50	2.39	2.40	2.60	2.50	2.39	2.41			
InSAR (cm)	2.68	2.68	2.69	2.69	2.57	2.68	3.18	2.47	2.57	2.68	2.72			
Weighted Misfit (cm)	2.45	2.45	2.45	2.45	2.51	2.45	2.56	2.57	2.51	2.45	2.47			
Temperature (°C)	20.30	20.30	20.30	20.30	20.27	20.30	20.28	20.37	20.35	20.30	20.38			

**Supplementary Table 10. Misfits of model predictions with different permeabilities of the normal-slip fault to surface displacement and temperature observations.**

**I. RMS misfits to Leveling observations (cm)**

Permeability		Horizontal		
		10 mD	20 mD	30 mD
Vertical	10 mD	2.78	2.89	3.02
	20 mD	3.37	2.39	2.64
	30 mD	2.74	2.80	2.98

**II. RMS misfits to InSAR observations (cm)**

Permeability		Horizontal		
		10 mD	20 mD	30 mD
Vertical	10 mD	2.74	4.14	2.50
	20 mD	2.68	2.68	2.57
	30 mD	3.57	2.53	2.75

**III. Weighted RMS misfits of deformation (cm)**

Permeability		Horizontal		
		10 mD	20 mD	30 mD
Vertical	10 mD	2.77	3.14	2.92
	20 mD	3.23	2.45	2.63
	30 mD	2.91	2.75	2.93

**IV. RMS misfits to well temperature (°C)**

Permeability		Horizontal		
		10 mD	20 mD	30 mD
Vertical	10 mD	20.69	21.04	21.03
	20 mD	20.56	20.30	20.74
	30 mD	23.03	20.89	20.33

**Supplementary Table 11. Misfits of model predictions with different thicknesses and properties (porosity, thermal conductivity and specific heat) of the plate boundary fault to surface displacement and temperature observations.**

RMS misfit	Thickness (m)			Porosity (%)			
	50	100	150	1	3	5	7
Leveling (cm)	3.03	2.39	3.15	2.72	2.59	2.39	2.56
InSAR (cm)	2.66	2.68	3.19	2.55	2.67	2.68	2.84
Weighted Misfit (cm)	2.96	2.45	3.16	2.69	2.61	2.45	2.62
Temperature (°C)	21.93	20.30	20.88	20.70	20.61	20.30	20.57
RMS misfit	Thermal Conductivity (W/(m·°C))				Specific heat (J/(kg·°C))		
	0.5	1	2	3	900	1000	1100
Leveling (cm)	2.39	2.39	2.39	2.39	2.39	2.39	2.39
InSAR (cm)	2.68	2.68	2.68	2.68	2.68	2.68	2.68
Weighted Misfit (cm)	2.45	2.45	2.45	2.45	2.45	2.45	2.45
Temperature (°C)	20.30	20.30	20.30	20.30	20.30	20.30	20.30

**Supplementary Table 12. Misfits of model predictions with different permeabilities of the plate boundary fault to surface displacement and temperature observations.**

**I. RMS misfits to Leveling observations (cm)**

Permeability		Horizontal		
		1 mD	5 mD	10 mD
Vertical	1 mD	3.38	2.71	2.83
	5 mD	2.97	2.39	3.05
	10 mD	2.60	2.45	3.11

**II. RMS misfits to InSAR observations (cm)**

Permeability		Horizontal		
		1 mD	5 mD	10 mD
Vertical	1 mD	4.25	3.12	3.05
	5 mD	4.29	2.68	2.51
	10 mD	2.80	2.84	2.65

**III. Weighted RMS misfits of deformation (cm)**

Permeability		Horizontal		
		1 mD	5 mD	10 mD
Vertical	1 mD	3.55	2.79	2.87
	5 mD	3.23	2.45	2.94
	10 mD	2.64	2.53	3.02

**IV. RMS misfits to well temperature (°C)**

Permeability		Horizontal		
		1 mD	5 mD	10 mD
Vertical	1 mD	20.59	20.63	20.56
	5 mD	20.57	20.30	20.71
	10 mD	20.83	20.59	20.70

**Supplementary Table 13. Misfits of model predictions with different thicknesses and properties (porosity, thermal conductivity and specific heat) of the subsidiary fault to surface displacement and temperature observations.**

RMS misfit	Thickness (m)			Porosity (%)		
	50	100	150	18	20	22
Leveling (cm)	3.16	2.39	3.57	2.80	2.39	2.87
InSAR (cm)	2.84	2.68	2.65	2.78	2.68	3.04
Weighted Misfit (cm)	3.10	2.45	3.39	2.80	2.45	2.90
Temperature (°C)	21.72	20.30	20.75	21.63	20.30	20.74
RMS misfit	Thermal Conductivity (W/(m·°C))			Specific heat (J/(kg·°C))		
	0.5	1	2	900	1000	1100
Leveling (cm)	2.39	2.39	2.39	2.39	2.39	2.50
InSAR (cm)	2.68	2.68	2.73	2.73	2.68	2.57
Weighted Misfit (cm)	2.45	2.45	2.46	2.46	2.45	2.51
Temperature (°C)	20.30	20.30	20.30	20.29	20.30	20.27

**Supplementary Table 14. Misfits of model predictions with different permeabilities of the subsidiary fault to surface displacement and temperature observations.**

**I. RMS misfits to Leveling observations (cm)**

Permeability		Horizontal		
		10 mD	20 mD	30 mD
Vertical	10 mD	2.85	3.34	3.22
	20 mD	2.29	2.39	2.97
	30 mD	2.73	2.96	3.16

**II. RMS misfits to InSAR observations (cm)**

Permeability		Horizontal		
		10 mD	20 mD	30 mD
Vertical	10 mD	2.64	3.01	2.62
	20 mD	3.08	2.68	2.99
	30 mD	2.77	2.79	2.61

**III. Weighted RMS misfits of deformation (cm)**

Permeability		Horizontal		
		10 mD	20 mD	30 mD
Vertical	10 mD	2.81	3.27	3.1
	20 mD	2.45	2.45	2.97
	30 mD	2.74	2.93	3.05

**IV. RMS misfits to well temperature (°C)**

Permeability		Horizontal		
		10 mD	20 mD	30 mD
Vertical	10 mD	21.20	20.60	20.67
	20 mD	20.76	20.30	20.57
	30 mD	20.78	21.03	21.09

**Supplementary Table 15. Misfits of model predictions with different scenarios of upwelling heat flux to surface displacement and temperature observations.**

Scenario I: RMS misfit	Heat fluid rate (kg/s)					
	1	5	10	20	50	100
Leveling (cm)	2.39	2.39	2.39	2.50	2.78	2.70
InSAR (cm)	2.73	2.73	2.68	2.73	2.79	3.12
Weighted Misfit (cm)	2.46	2.46	2.45	2.55	2.78	2.78
Temperature (°C)	20.30	20.30	20.30	20.30	20.34	20.63
Scenario II: RMS misfit	Heat fluid rate (kg/s)					
	1	5	10	20	50	100
Leveling (cm)	2.48	2.48	2.49	2.49	2.50	2.58
InSAR (cm)	2.76	2.76	2.75	2.75	2.73	2.64
Weighted Misfit (cm)	2.54	2.54	2.54	2.54	2.55	2.59
Temperature (°C)	20.27	20.27	20.27	20.27	20.30	20.60

Scenario I: only the normal-slip fault serving as the heat conduit; Scenario II: both of the normal-slip fault and strike-slip subsidiary fault serving as the conduit.

**Supplementary Table 16. Misfits of model predictions with different properties of water to surface displacement and temperature observations.**

RMS misfit	Density (kg/m <sup>3</sup> )			Viscosity (Pa·s)				Compressibility (Pa <sup>-1</sup> )		
	800	900	1000	1.5×10 <sup>-4</sup>	2×10 <sup>-4</sup>	2.5×10 <sup>-4</sup>	3×10 <sup>-4</sup>	3.7×10 <sup>-10</sup>	4.2×10 <sup>-10</sup>	4.7×10 <sup>-10</sup>
Leveling (cm)	2.42	2.65	2.39	3.39	2.57	2.39	3.03	3.67	2.39	3.18
InSAR (cm)	3.39	2.60	2.68	2.58	2.84	2.68	2.59	4.20	2.68	2.79
Weighted Misfit (cm)	2.61	2.64	2.45	3.23	2.62	2.45	2.94	3.78	2.45	3.10
Temperature (°C)	20.36	20.30	20.30	20.69	20.42	20.30	21.21	20.42	20.30	20.96
RMS misfit	Thermal Conductivity (W/(m·°C))			Specific Heat (J/(kg·°C))						
	0.58	0.68	0.78	3900	4200	4500	4800			
Leveling (cm)	2.39	2.39	2.39	2.66	2.39	2.62	2.80			
InSAR (cm)	2.68	2.68	2.68	2.51	2.68	2.41	2.99			
Weighted Misfit (cm)	2.45	2.45	2.45	2.63	2.45	2.58	2.84			
Temperature (°C)	20.30	20.30	20.30	20.55	20.30	20.53	20.44			

**Supplementary Table 17. Variations of RMS misfits of displacement and temperature in model calibration.**

Formation	Parameter	Variation of RMS misfit <sup>a</sup>	
		Displacement	Temperature
Reservoirs	Porosity	33%	10%
	Permeability of the upper reservoir	31%	6%
	Permeability of the lower reservoir	36%	7%
	Biot coefficient	2%	0
	Thermal expansion coefficient	16%	0
	Thermal conductivity	8%	1%
	Specific heat	17%	3%
Feeder fault	Thickness	22%	4%
	Porosity	16%	2%
	Permeability	24%	12%
	Young's modulus	0	0
	Poisson's ratio	0	0
	Thermal expansion coefficient	0	0
	Thermal conductivity	5%	1%
Boundary fault	Specific heat	2%	0
	Thickness	23%	7%
	Porosity	9%	2%
	Permeability	31%	3%
	Thermal conductivity	0	0
Subsidiary fault	Specific heat	0	0
	Thickness	28%	7%
	Porosity	16%	6%
	Permeability	25%	4%
	Thermal conductivity	0	0
	Thermal conductivity	0	0
	Specific heat	2%	0

<sup>a</sup>The variation are calculated with the RMS misfits of simulated surface displacement and reservoir temperature to observations (Supplementary tables 4-14) based on the expression,  $(R_{max} - R_{min})/R_{max}$ , where  $R_{max}$  and  $R_{min}$  are the maximum and minimum RMS misfits, respectively.